E. WOLF, PROGRESS IN OPTICS VVV

X

COHERENT BACKSCATTERING AND ANDERSON LOCALIZATION OF LIGHT *

BY

Christof M. Aegerter
Fachbereich Physik,
Universität Konstanz,
Universitätstrasse 10,
78457 Konstanz
Germany

Georg Maret
Fachbereich Physik,
Universität Konstanz,
Universitätstrasse 10,
78457 Konstanz
Germany

*Version August 8, 2007

CONTENTS[1]

[1]Run LaTeX twice for up-to-date contents.

§ 1. Introduction

Most of the time, we obtain information on an object by looking at it, that is we exploit the light that is scattered from it. The spectral and angular distribution of the backscattered (and reflected) light gives us information about the nature of the particles making up the object. For instance the redish colour of copper is determined by the absorption properties (in the green) of the d electrons in the partially filled shell. On the other hand, the blue colour of the sky is well known to originate from the scattering properties of the air molecules which follows Rayleigh scattering with a cross-section proportional to $1/\lambda^4$. This tells us that the molecules are much smaller than the wavelength of light. In fact a more thorough analysis allows a characterization of the density fluctuations of the air from the scattering properties of the sky. As a final example, we mention the 'Glory', the halo seen around the shadow of an airplane on the clouds when flying on an overcast day, which will be discussed further below. In the following, we will be concerned with instances of such enhanced backscattering in nature, where the intensity is enhanced in the direction of backscattering. As we will see below, one such effect is due to an interference of multiple scattering paths in disordered media like clouds, milk or white paint. Due to reciprocity of light propagation, such paths will always have a counterpart of exactly the same length, which implies that they will always interfere constructively in the backward direction.

We will also discuss below, that this effect can lead to a marked change in the transport behaviour of the light waves in a disordered system, where diffuse transport comes to a halt completely. This transition is known as Anderson localization and has had a great influence in the development of the theory of electrons in metals and condensed matter physics. However, as seen by the backscattering enhancement discussed below, the effect is also present in classical waves such as light and there have been great efforts to try and experimentally observe the transition to Anderson localization of light.

In the rest of the introduction, we will discuss the different instances of enhanced backscattering in nature and their possible connection to coherent backscattering. Then we will discuss the connection of coherent backscattering to Anderson localization in more detail, before discussing the main predictions of Anderson localization in order to guide the experimental search for the effect.

Section 2 will return to coherent backscattering and will discuss in detail

the different experimental observations connected to recurrent scattering, the influence of absorption and finite size of the medium, as well as the problem of energy conservation. In this section, we will also discuss other instances of coherent backscattering, i.e. that observed from light scattered by cold atoms as well as that observed with waves other than light.

In section 3 we will discuss the quest for Anderson localization of light, where we describe the different experimental approaches used in the past, as well as their advantages and disadvantages. In the end, we will concentrate on our recent studies of time-resolved transmission and the corresponding determination of critical exponents of Anderson localization of light.

1.1. INSTANCES OF ENHANCED BACKSCATTERING

As first realized by Descartes [1637], the rainbow is an enhancement in intensity (different for different colours due to dispersion) due to refraction of light in the rain drops, which due to the dispersion of water is highest at different angles for different colours. However, this is a purely geometric effect, which does not yield information on the size of the rain drops reflecting the light. Something akin a rainbow can be seen when flying in an airplane over an overcast sky. When the sun is low and the cloud cover not too thick, one can see a beautiful halo around the shadow of the plane on the clouds. The effect is also well-known to alpinists who can observe this halo around their own shadow on a day which is hazy is the valley. In contrast to what one might think, this 'Glory' as it is called, is not in fact a rainbow. One can see this for instance by considering the angle of this colourful enhancement, which is usually only a few degrees and hence much smaller than the 42° corresponding to a rainbow. Therefore another mechanism has to be at work. It has been shown that the size of the scattering droplets influences the angle of the glory (Bryant and Jarmie [1974]). It turns out, that this is due to the properties of Mie-scattering (Mie [1908]) of the droplets. With a typical size of 10μm, the droplets in a cloud are large compared to the wavelength of light. Furthermore, as illustrated by experiments on a levitating droplet of water the Glory is the property of a single drop (Lenke, Mack, and Maret [2002]).

Enhanced backscattering is also commonly observed in forests, where the leaves of dew-covered trees, or the blades of dew-covered grass have a halo. This effect is called sylvanshine (see e.g. Fraser [1994]) and is due to the focussing action of the droplet onto the reflecting surface of the leaf. By the same principle, the diffuse reflection from the leaf is channelled back

through the lens (i.e. the drop) which decreases the angle of reflection. Hence the leaves or the grass is brighter than the background. The grass even need not be dew-covered to observe a halo, as there is an additional effect increasing the intensity in the direct backscattering direction. Exactly opposite to the incidence, any ensemble of rough objects will be brightest. This is because in this direction, we directly see the reflected light and none is lost due to shadows of other objects (Fraser [1994]). This is known as the corn-field effect.

As a final instance of enhanced backscattering, let us mention the observation of the intensity of objects in the solar systems, such as the moon or other satellites of planets, when the earth and the sun are in opposition to the moon. In that case, it was observed by Gehrels [1956] for the moon and subsequently for many other satellites (Oetking [1966]) that the intensity of the satellite is in fact increased over its usual value. Due to the arrangement of sun and satellite when the effect is observed, this was called the 'opposition effect'. In this effect, coherent backscattering as we will discuss it below goes together with analogues of effects above, such as the corn-field effect. The presence of coherent backscattering in the opposition effect was only recently discovered (Hapke, Nelson and Smythe [1993]). With this knowledge it was then possible to actually study the surface properties (e.g. the granularity) of these satellites from remote observations.

1.2. COHERENT BACKSCATTERING

Among instances of enhanced backscattering, we will here be concerned mostly with coherent backscattering, which is an interference effect that survives all averages in a random medium. Fundamentally, the enhancement is due to the fact that because of time-reversal symmetry, every path through a random medium has a counterpropagating partner. Light elastically scattered on these two paths interferes constructively, because the pathlengths are necessarily the same. This leads to an enhancement of exactly a factor of two in the direction directly opposite the incidence. In contrast to the glory or other effects discussed above (Lenke, Mack, and Maret [2002]), coherent backscattering is not an interference due to the properties of a single scatterer, but relies fundamentally on multiple scattering. In fact in the single scattering regime, there cannot be a coherent backscattering cone as there cannot be a counterpropagating light path. The entry- and exit-point of a multiple scattering path can then be seen as the two points of a double-slit, which due to the coherence of

the time-reversed paths necessarily interfere with each other. The different interference patterns corresponding to different light paths in the disordered medium have to be averaged over, which will lead to the shape of the backscattering cone discussed in Sec. 1.3 below. What can be seen from this picture is that in the exact backscattering direction, the averaging will always lead to an enhancement factor of two.

These principles behind the origin of the backscattering cone will strongly influence the transport through a random system. Taking the end points of the counterpropagating paths to coincide somewhere inside the sample, there will be a twofold enhancement at this point on such a closed loop. This in turn leads to a decreased probability of transport through the system. This effect is what causes Anderson localization of light (Anderson [1958]), i.e. the loss of diffuse transport due to increasing disorder. As disorder increases, the probability of forming closed loops on which intensity is enhanced increases. At a certain critical amount of disorder, these closed loops start to be macroscopically populated, which leads to a loss of diffuse transport. This critical amount of disorder as been estimated by dimensional arguments by Ioffe and Regel [1960] to be when the mean free path roughly equals the inverse wave-number, i.e. when $kl^* \sim 1$. Such a mechanism was first proposed for the transport of electrons in metals, where it was found that an increase in disorder can turn a metal into an insulator (see e.g. G. Bergmann [1984]).

The first instances of localization were discussed in the context of electron transport in metals, and thus localization was thought to be a quantum effect. Moreover, due to the fact that localization should always be present in two dimensions (see scaling theory below) and is not influenced too much by the presence of correlations, these studies were carried out in thin films. A review of these experiments can be found in Altshuler and Lee [1988], G. Bergmann [1984] and these studies of localization in lower dimensions have had a big influence on other quantum effects in low dimensional electron systems such as in the quantum Hall effect (Klitzing, Dorda, and Pepper [1980], Laughlin [1983]).

Eventually it was however realized that the quantum nature of electrons is not a necessary ingredient for the occurrence of Anderson localization as, in fact, this was a pure wave effect. This implied that it should also be possible to observe localization effects with classical waves, such as light as was proposed by John [1984] and Anderson [1985]. As we will see below, shortly thereafter, coherent backscattering, i.e. weak localization was observed with light and subsequently, there was a vigorous programme to

also observe signs of strong localization of light, because the study of photon transport in disordered media has many advantages over the study of electrons in metals. This is because in the latter case, possible alternatives may lead to localization as well: In the case of electrons, a random potential can lead to a trapping of particles, which also strongly affects transport, while not being connected to localization. On the other hand, electrons also interact with each other via Coulomb interaction, such that correlations in electron transport are again not necessarily due to localization effects, but are more likely explained by electron-electron interactions. In fact it can be shown that in the presence of particle interactions, the effects of localization vanish (Lee and Ramakrishnan [1985]).

However, as we will discuss below, the photonic system is not completely free of possible artifacts masking as localization. For instance, light will be absorbed by materials to a certain extent, which leads to a loss of energy transport similar to localization. Furthermore, resonant scattering can lead to a time delay in the scattering process, which leads to a slowing down of transport, which again may be mistaken for localization. In Sec. 3 below, we will discuss in detail how these possible artifacts can be circumvented and localization can in fact be observed.

1.3. THEORETICAL PREDICTIONS

As discussed above, the enhanced backscattering from turbid samples known as coherent backscattering is a manifestation of weak localization of light. In electronic systems, localization was intensely studied and many of the predictions found there can be applied also to optics. Here we will discuss the most prominent predictions, which will also serve as a guiding line in the quest to observe Anderson localization of light. Most prominent in these are the predictions of the change in static transmission (Anderson [1985], John [1984]) which turned out to be difficult to observe experimentally due to the presence of absorption in real samples. The critical prediction for Anderson localization concerns the fact that there should be a phase transition to a state where diffusion comes to a halt. This is described by scaling theory (Abrahams, Anderson, Licciardello, and Ramakrishnan [1979]), which can also be investigated by a self-consistent diagrammatic theory (Vollhardt and Wölfle [1980]). This version of the theory can also be extended to describe open systems with absorption, a situation much more adjusted to describe experiments (Skipetrov and van Tiggelen [2004], Skipetrov and van Tiggelen [2006]). First of all, we will however describe

the shape of the backscattering cone as calculated by Akkermans, Wolf, and Maynard [1986], van der Mark, van Albada, and Lagendijk [1988].

1.3.1. The cone shape

Given the nature of the backscattering cone due to interference of photons on time-reversed paths, one can explicitly calculate the shape of the enhancement as a function of angle. In order to do this, the interference patterns corresponding to two counterpropagating paths with end-to-end distance ρ need to be averaged weighted by the probability distribution of such an end-to-end distance occurring. Like in a double slit experiment with slit separation ρ, each of these interference patterns will contribute a factor $1 + \cos(q\rho)$, such that the enhancement above the incoherent background is simply given by the real part of the Fourier transform of the end-to-end distance distribution.

$$\alpha(q) = \int p(\rho) \cdot \cos(q\rho)\, d\rho \tag{1.1}$$

In the diffusion approximation, this probability distribution can be calculated (Akkermans, Wolf, Maynard and Maret [1988], van der Mark, van Albada, and Lagendijk [1988]) to be $1/a(1 - \rho/\sqrt{\rho^2 + a^2})$in the case of a semi-infinite planar half-space. Here, the length scale $a = 4\gamma l^*$ describes how the diffuse intensity penetrates the sample as described by the Milne parameter γ and the transport mean free path l^*. The parameter γ can be calculated from the radiative transfer equation to be $\sim$0.71 and in the diffusion approximation is exactly $\gamma = 2/3$. In the following, we will always use the value of $\gamma = 2/3$. This leads to an expression for the backscattering enhancement of

$$\alpha(q) = \int \left(1 - \frac{\rho}{\sqrt{\rho^2 + a^2}}\right) \cdot \cos(q\rho)\, d\rho, \tag{1.2}$$

which can be solved to give (Akkermans, Wolf, and Maynard [1986], Akkermans, Wolf, Maynard and Maret [1988], van der Mark, van Albada, and Lagendijk [1988]):

$$\alpha(q) = \frac{3/7}{(1 + ql^*)^2} \left(1 + \frac{1 - \exp(-4/3ql^*)}{ql^*}\right) \tag{1.3}$$

This gives a cone shape which is in very good agreement with the experiments discussed in Sec. II below. As can be seen from an investigation

of the angle dependence, the cone tip is triangular with an enhancement of 1 in the exact backscattering direction. The enhancement then falls off on an angular scale proportional to $1/kl^*$, in fact the full width at half maximum of the curve is given by $0.75/(kl^*)$. Thus the investigation of the backscattering cone is a very efficient method of determining the turbidity of a sample as given by $1/l^*$.

A similar description following diagrammatic theory, where the most crossed diagrams have to be added up, was also given by Tsang and Ishimaru [1984]. The main features of the curve remain the same, however the different theories use different approximations for the Milne parameter.

1.3.2. Static transmission

One of the main predictions of Anderson localization in electronic systems is the transition from a conducting to an insulating state. This of course has strong implications on the transmission properties of localized and non-localized samples. For a conducting sample, the transmission is described by Ohm's law, which describes diffusive transport of particles and hence a decrease of transmission with sample thickness as $1/L$. This is also the case in turbid optical samples, where the transmission in the diffuse regime is simply given by $T(L) = T_0 l^*/L$ (see e.g. Akkermans and Montambaux [2006]). In the presence of absorption, this thickness dependence of the total transmission will change to an exponential decay for thick samples according to

$$T(L) = T_0 \frac{l^*/L_a}{\sinh(L/L_a)}, \tag{1.4}$$

where $L_a = \sqrt{l^* l_a/3}$ is the sample absorption length corresponding to an attenuation length l_a of the material, which describes the absorption of the light intensity along a random scattering path.

The localization of photons will similarly affect the transmission properties of a sample. As the diffusion coefficient of light becomes scale dependent close to the transition to localization, the total transmission will decrease. Scaling theory of localization discussed below predicts that the diffusion coefficient at the transition will decrease as $1/L$ (John [1984]). This should then be inserted into the expression for the diffuse transmission of the sample resulting in a different thickness dependence $T(L) \propto 1/L^2$. Again, this ignores the effects of absorption and Berkovits and Kaveh [1987] have calculated the effects of absorption in the presence of a renormalized

diffusion coefficient, where they find:

$$T(L) = T_0 \exp(-1.5L/L_a) \tag{1.5}$$

Again, this leads to an exponential decrease of the transmitted intensity for very thick samples, where however the length scale of the exponential decrease is changed. When photons are fully localized, the transport is exponentially suppressed, as only the tails of the localized intensity can leave the sample. Thus Anderson [1985] has predicted the transmission in the localized case to be given by $T(L) = T_0 \exp(-L/L_{loc})$, where L_{loc} describes the length scale of localization. As was the case above, this derivation again does not take into account absorption and a fuller description would be given by

$$T(L) = T_0 \frac{l^*/L_a}{\sinh(L/L_a)} \exp(-L/L_{loc}). \tag{1.6}$$

Again, this gives an exponential decrease of the transmitted intensity for thick samples with an adjusted length scale not solely given by the absorption length L_a. In an experimental investigation of Anderson localization therefore, static transmission measurements will have to find an exponential decrease of the transmission that is faster than that given by absorption alone. This implies that the absorption length must be determined independently for such an investigation to be able to indicate localization of light.

1.3.3. Scaling theory

When studying the thickness dependence of the conductance (i.e. the transmission), its dependence on disorder has to be taken into account. Abrahams, Anderson, Licciardello, and Ramakrishnan [1979] produced a first version of such a theory, where they introduce the 'dimensionless conductance', g as the relevant parameter to study. In electronic systems, this simply is the measured conductance normalized by the quantum of conductance, e^2/h. In optics, the conductance is naturally dimensionless and can be defined simply via the transmission properties of the sample. In fact, g can be calculated in three dimensions from the ratio of the sample volume to that occupied by a multiple scattering path. This volume of the multiple scattering path is given by $\lambda^2 s$, where s is the length of the path, which in the case of diffusion is $s \propto L^2/l^*$. Thus one obtains $g \simeq (W/L)(kW)(kl^*)$, where W is the width of the illumination, which could also be obtained from the static transmission discussed above. In the

case of a localized sample, the transmission decreases exponentially with L, which has to be reflected in a renormalization of the path lengths in order to give an exponentially decreasing g. Abrahams, Anderson, Licciardello, and Ramakrishnan [1979] main ansatz in treating the problem of the localization transition in the following is to suppose that the logarithmic derivative $\beta = \mathrm{d}(\ln g)/\mathrm{d}(\ln L)$ can be expressed as a function of g only.

The transition to a localized state is then given by the criterion that β changes from a positive value to a negative one. Ohm's law as a function of dimensionality states that the conductance scales as $g \propto L^{d-2}$. Therefore, making a sample larger and larger in low dimensional systems will in fact lead to a reduction of the conductance and hence be associated with localization. Actually Ohm's law straightforwardly implies that $\beta = d - 2$ for large L (and thus g), such that $d = 2$ is the lower critical dimension for a transition to localization to occur. In fact, for low dimensional systems the waves are always localized (Abrahams, Anderson, Licciardello, and Ramakrishnan [1979]).

Where there is a transition to localization (i.e. in $d > 2$), more details about that transition can be obtained by assuming the dependance of β on g to be linear at the crossing of the null-line. In this case, the scaling function β describes how one arrives from a diffuse conductance to one which is exponentially suppressed in the localization length. This transition is a function of the disorder in the system, such that one can describe it in terms of a diverging length scale of localization at the transition. This would be given by an exponent ν, such that $L_{loc} \propto |(g - g_c)/g_c|^{-\nu}$. In the assumption that close to the transition, β can be approximated by a linear function in $\ln g$, this exponent is simply given by the inverse slope of β at the transition. In the framework of scaling theory, no exact value can be given for this exponent, however extrapolating β from its known dependencies at large and small disorder, Abrahams, Anderson, Licciardello, and Ramakrishnan [1979] obtain an upper bound of $\nu < 1$. As a matter of fact, John [1984] has shown that expanding the treatment around the lower critical dimension, the exponent should be given by $\nu = 1/2$ in $d = 2 + \epsilon$ dimensions. Such a value for the critical exponent would also be expected for $d > 4$, where it should simply be given by the mean field value of a critical exponent of an order parameter (Schuster [1978]).

At the transition, the loss of transmission can be described by a scale dependence of the diffusion coefficient, such that D becomes smaller as the sample size L increases. As discussed above this results in $D \propto 1/L$. Such a scale dependent diffusion coefficient can however also be described in the

time domain, where the scale dependence corresponds to a decrease of D with increasing path length. To quantify this, one has to insert the scale dependent D into the diffuse spread of the photon cloud: $\langle r^2 \rangle = Dt$. Since D depends on the length scale as $1/L$, we obtain that $D \propto t^{-1/3}$ at the transition (Berkovits and Kaveh [1990]). For states which are localized, i.e. with an exponential decrease of the transmission, the spread of the photon cloud has to be limited to the length-scale of L_{loc}, such that in this case we obtain $D \propto 1/t$. Such a time dependent diffusion coefficient will constitute the hall-mark of Anderson localization and can also be described by self-consistent theories, which predict the temporal scaling of D (Vollhardt and Wölfle [1980]). These theories have been adapted to a semi-infinite, open medium in order to describe the influence of localization on the coherent backscattering cone by van Tiggelen, Lagendijk, and Wiersma [2000]. They obtain a rounding of the cone, which experimentally is difficult to distinguish from absorption. Subsequently, Skipetrov and van Tiggelen [2004], Skipetrov and van Tiggelen [2006] have applied self-consistent theory to open slabs, which are comparable to an experimental situation. Here they indeed find that in time-resolved experiments, a measure of $D(t)$ could be found that can be studied experimentally. Will will describe this in detail below.

§ 2. Experiments on coherent backscattering

As we have seen above, the enhancement of backscattered light is due to the wave-nature of light and time-reversal symmetry (or reciprocity) of the wave propagation. As such it is an illustration of the principle behind Anderson localization. Since light does not interact with itself and thus correlation effects can be ruled out, there have been numerous experiments on coherent backscattering of light - and other waves - in order to study directly the influence of disorder, polarization and the scattering process on Anderson localization. In this section, we will discuss these experiments starting with the discovery of coherent backscattering and continuing with other influential factors, such as sample thickness and absorption. Then we will discuss the effects of increased disorder on the backscattering cone before discussing experiments on multiple scattering in clouds of cold atoms. There, the nature of the scattering process is of paramount importance and the symmetries responsible for backscattering can be broken due to internal degrees of freedom of the atom involved in the scattering process. Finally we describe some experiments on coherent backscattering using waves other than light, such as acoustic and matter waves.

2.1. COLLOIDAL SUSPENSIONS AND TURBID POWDERS

Soon after the prediction was made by John [1984] and Anderson [1985] that Anderson localization may be observed with light waves, weak localization was observed in the backscattering from colloidal suspensions by van Albada and Lagendijk [1985] as well as by Wolf and Maret [1985]. These two groups used slightly different setups to study suspensions of polystyrene particles, see Fig. 1. van Albada and Lagendijk [1985] illuminated their sample using a beam splitter, such that the backscattered light can be directly observed using a photomultiplier on a translation stage. In present comparable setups, a CCD camera is used to capture the backscattered light. Wolf and Maret [1985] on the other hand illuminated the sample using a glass slide used as a beam splitter and placed the detector on a goniometer.

As can be seen from inspection of figure 2, they both obtain very similar results. Increasing the volume fraction of polystyrene particles (i.e. decreasing l^*), the observed backscattering cone gets wider. In both cases, sizeable enhancement factors are found, however still far from the ideal value of 1 predicted theoretically. This is due to the fact that the setups

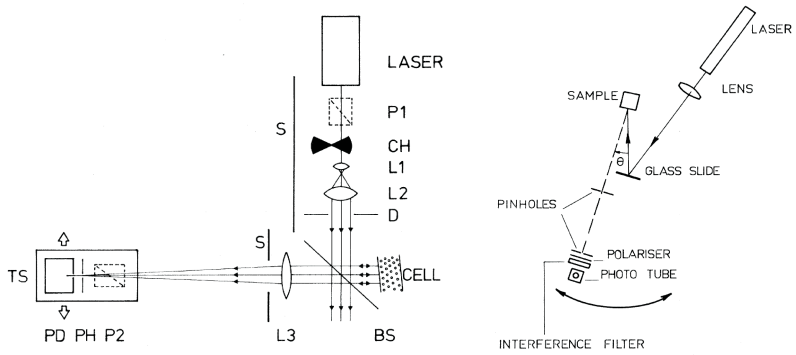

Figure 1: The different setups used by van Albada and Lagendijk [1985] (left) and Wolf and Maret [1985] (right) to measure backscattering cones (see text). Reprinted figure with permission from van Albada and Lagendijk [1985] and Wolf and Maret [1985]. Copyright 1985 by the American Physical Society.

lacked angular resolution very close to the center, as well as a residual effect of direct reflection which is not suppressed completely. These problems were later on solved in the setups discussed below.

An enhancement of backscattered light was also found by Tsang and Ishimaru [1984], Kuga and Ishimaru [1984], however the enhancements there were much smaller than those discussed above. Furthermore, both van Albada and Lagendijk [1985], as well as Wolf and Maret [1985] have discussed their findings in the context of weak localization, which was not the case in Kuga and Ishimaru [1984].

Random interference of photons on multiply scattered paths can lead to very large fluctuations in the intensity. These fluctuations are called a speckle pattern. In order to observe a coherent backscattering cone at all, the fluctuations due to the speckle pattern need to be averaged. Using a colloidal suspension, as carried out by van Albada and Lagendijk [1985], Wolf and Maret [1985], this averaging is achieved by the motion of the scatterers, which leads to a redistribution of the pathlengths. In fact, studying the decrease of the time auto-correlation of a speckle spot directly gives information of the motion of the scatterers. This was developed into the technique known as diffusing wave spectroscopy by Maret and Wolf [1987], Pine, Weitz, Chaikin, and Herbolzheimer [1988] to extract

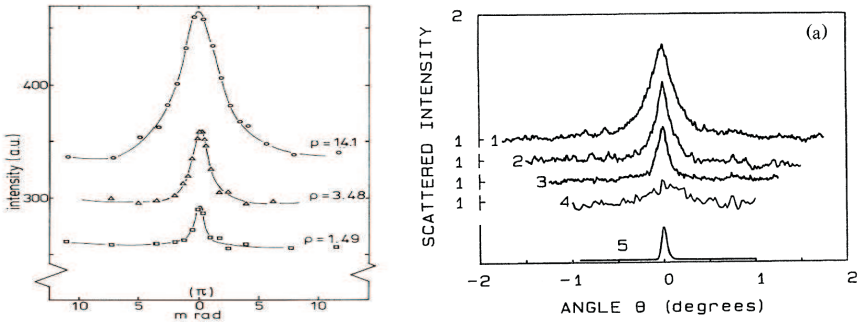

Figure 2: The dependence of the backscattering cones on the density of suspended particles (i.e. the mean free path). On the left, the data of van Albada and Lagendijk [1985] are shown with densities varying from 1.4 10^{17} to 1.4 10^{16} m^{-3} and beads of a diameter of 1.09 μm. On the right, corresponding data of Wolf and Maret [1985] are shown, where the volume fractions change from 0.004 to 0.11 and beads of a diameter of 0.49 μm. Due to limited angular resolution, stray light and single backscatterig contributions, the enhancements are between 0.4 and 0.6. Reprinted figure with permission from van Albada and Lagendijk [1985] and Wolf and Maret [1985]. Copyright 1985 by the American Physical Society.

information on particle size, flow rates and relaxation dynamics in complex turbid fluids. In turbid powders, the averaging over the speckle pattern is usually done by rotating the sample, which leads to a configurational average (see e.g. Gross, Störzer, Fiebig, Clausen, Maret, and Aegerter [2007]).

2.1.1. Experimental setups for large angles

In order to be able to characterize highly turbid samples in addition to the relatively dilute suspensions discussed above, an apparatus capable of resolving rather large angles is needed. A rough estimate of the angles needed for samples close to the Ioffe-Regel criterion (Ioffe and Regel [1960]) results in a cone width of up to 40°. Even taking into account the narrowing of the cone due to internal reflections at the surface (see below) this means that in order to properly determine the level of the incoherent background, angles up to at least 40° need to be measured. However at the same time, the setups should be able to resolve the cone-tip with great accuracy in order to observe deviations from the ideal tip shape (see below). These two requirements pose a big challenge, which have been solved to some extent (angles up to 25°) by Wiersma, van Albada, and Lagendijk [1995] and Gross, Störzer, Fiebig, Clausen, Maret, and Aegerter [2007] (angles up to 85°) in two very different ways.

The setup of Wiersma, van Albada, and Lagendijk [1995] combines a movable detector with the method of using a beam splitter to be able to observe the most central angles to high accuracy. Instead of just moving the arm of the detector, an ingenious scheme is used whereby the sample, detector and beamsplitter are moved in concert to ensure that the detected light is always perpendicular to the detector and the incident light is always perpendicular to the sample surface. This is to ensure that the polarizer (P in figure 3) is always arranged such that direct reflections are extinguished completely. The angular range covered by the setup is however limited by the presence of the beam splitter to below 45°, such that the incoherent background in extremely wide cones cannot be assessed. On the other hand, a single setup can cover all angles up to 25° at almost unlimited resolution with an extinction rate for singly reflected light of nearly 100 %.

A radically different approach was chosen by Gross, Störzer, Fiebig, Clausen, Maret, and Aegerter [2007]. Here, moveable parts are completely absent and the backscattered intensity is measured at all angles simultaneously. This is done via a set of 256 highly sensitive photodiodes placed

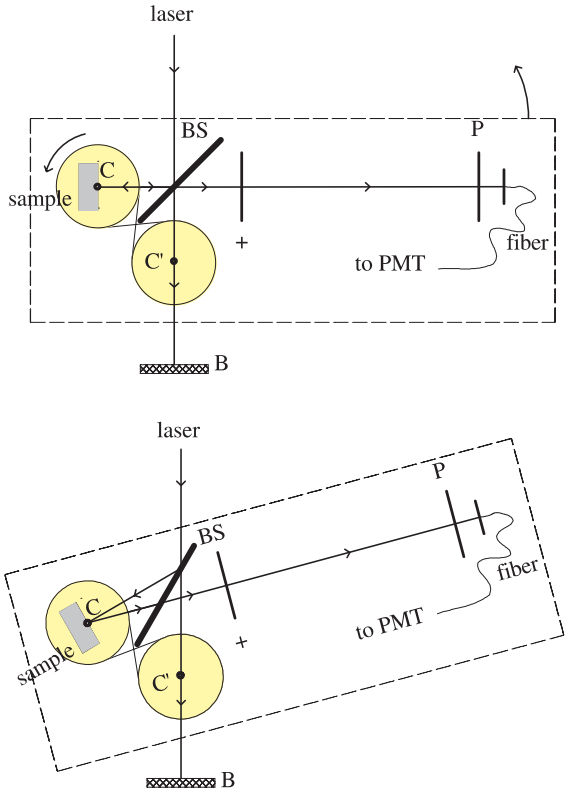

Figure 3: The wide angle setup of Wiersma, van Albada, and Lagendijk [1995]. The top and bottom figure show the setup at two different angles and illustrate the rotation of the sample, the beam splitter and the detector in concert in order to keep the incident light always perpendicular on the sample and the detected light always perpendicular on the detector. This is to reduce aberrations in the polarizer when the light is incident at an angle, such that enhancement factors of unity can actually be measured. Reprinted figure with permission from Wiersma, van Albada, and Lagendijk [1995]. Copyright 1995 by the American Physical Society.

around an arc of a diameter of 1.2 m. At the very center of the arc, photodiode-arrays are used which yield a limiting angular resolution of 0.14°. At higher angles, the diodes are increasingly spaced, such that at angles $> 60°$ the resolution is 3°. In addition, the central 3° of the cone are measured using a beam splitter and a CCD camera similar to those described above. This gives good overlap to the central part of the wide-angle apparatus, such that effectively the whole angular range is covered, while still measuring the tip of the cone with a resolution of 0.02°. The problems of perpendicular incidence onto the circular polarizers discussed above is solved by using a flexible polarizer foil, which is placed in front of the whole arc. Such a polymer based polarizer has the disadvantage that only about 96% of the reflected light is extinct, such that enhancements of 2 as obtained by Wiersma, van Albada, and Lagendijk [1995] are not possible with this setup. On the other hand, such a polarizer is much cheaper to obtain and can be used in a larger window of wavelengths than a linear polarizer and quarter-wave plate. For wave-length dependent studies this is a great advantage. Furthermore the renunciation on movable parts makes it possible to measure the small intensities at very large angles with reasonable accuracy.

In addition, very broad backscattering cones pose a problem in that they would seriously breech conservation of energy. As the total reflectivity of an infinitely thick, non-absorbing sample should be $R = 1$, the photon energy within the backscattering cone must be obtained from destructive interference at other scattering angles. In order to be able to tackle this problem experimentally, a calibrated energy scale would be needed. A simple extension of the setup of Gross, Störzer, Fiebig, Clausen, Maret, and Aegerter [2007] is capable of this, as will be described below.

2.1.2. Absorption and finite thickness

In all of the above, we have assumed that the sample can be treated as in infinite half-space, such that all incident photons are eventually backscattered at the sample surface. In reality, this is not always a good approximation and photons may either be absorbed or leave the sample on the other end or the sides. This implies that the photon pathlength distribution needs to be adjusted by suppressing such long paths. This can for instance be done by introducing an exponential cut-off to the probability distribution $p(s)$ discussed above. Therefore, we expect that the tip of the cone, corresponding to these long paths is altered. van der Mark, van Albada, and Lagendijk

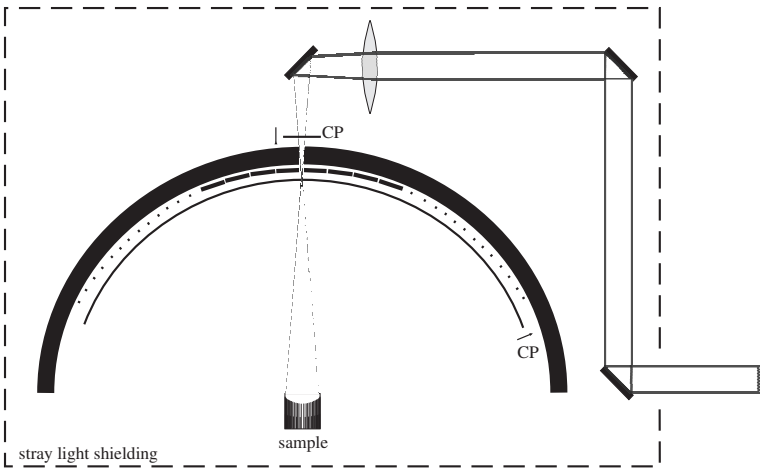

Figure 4: The wide-angle setup of Gross [2005]. The sample is at the center of an arc of 1.2 m diameter, which holds 256 sensitive photodiodes. At the center, the diodes are minimally spaces yielding a resolution of 0.14° and are increasingly spaced out to 85°. To shield ambient light, the whole setup is placed inside a black box. Direct reflections are suppressed by the use of circular polarization, which is achieved using a flexible polarization foil which is placed in front of the whole arc. With this, enhancement factors up to 0.96 are possible. The different diodes are calibrated using a teflon sample, which in this angular range gives a purely incoherent signal. Reprinted figure with permission from Gross, Störzer, Fiebig, Clausen, Maret, and Aegerter [2007]. Copyright 2007 by the American Physical Society.

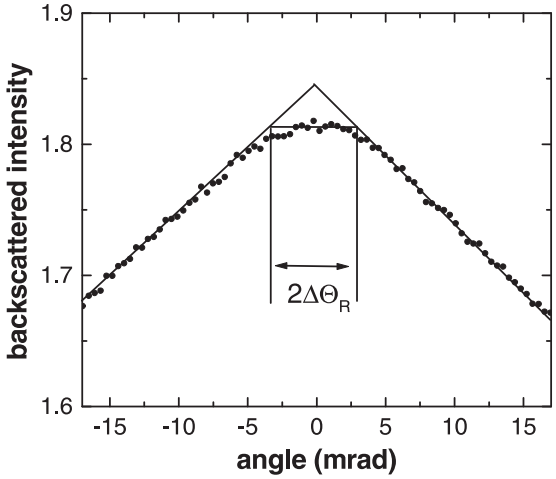

Figure 5: Absorption, finite thickness, but also localization of light would lead to a rounding of the cone-tip, which ideally would be linear as discussed above. This is because in all of these cases, photons on long paths are not reflected from the sample and therefore do not contribute to the backscattering cone. In these data from Schuurmans, Megens, Vanmaekelbergh, and Lagendijk [1999], this rounding can be clearly seen for a sample of photoanodically etched GaP. Due to the lack of an independent determination of the absorption length it is difficult to associate this rounding clearly with absorption or localization. Reprinted figure with permission from Schuurmans, Megens, Vanmaekelbergh, and Lagendijk [1999]. Copyright 1999 by the American Physical Society.

[1988], Akkermans, Wolf, Maynard and Maret [1988], Ishimaru and Tsang [1988] have studied this problem quantitatively and find that indeed, the tip of the cone is rounded. For the simple case of absorption, the cone shape can be obtained by replacing q in Eq. by $\sqrt{1/L_a^2 + q^2}$ (Akkermans, Wolf, Maynard and Maret [1988]), where L_a is the absorption length of the multiple scattering sample, i.e. $\sqrt{l^* l_a/3}$, where l_a is the absorption length of the material. This leads to a rounding on the angular scale of $\Delta\theta = 1/kL_a$. In the case of a finite sample, the situation is somewhat more complicated, but van der Mark, van Albada, and Lagendijk [1988] have derived that in that case, the rounding is on an angular scale of $\Delta\theta = \coth(L/L_a)/kL_a$.

Such a rounding of the cone has been observed by Wolf, Maret, Akkermans and Maynard [1988], Schuurmans, Megens, Vanmaekelbergh, and Lagendijk [1999], see e.g. figure 5. Similarly, the scaling of the width of the rounding with sample thickness L and absorption length L_a has been tested experimentally (see figure 24 below). However, from the discussion above it is also plausible that localization would lead to a rounding of the backscattering cone since localization too leads to a redistribution of the pathlengths for very long paths. This has been suggested by Berkovits and Kaveh [1987] and calculated using self consistent theory by van Tiggelen, Lagendijk, and Wiersma [2000]. We will discuss these issues further in the context of strong localization below.

2.1.3. Surface reflections

In the above discussion of the shape of the backscattering cone, we have assumed that the cone is directly given by the diffuse pathlength distribution of photons at the free sample surface. However, since samples usually have an effective refractive index higher than air, this distribution can be influenced by internal reflections of the light as it exits the sample. Such reflections will effectively broaden the pathlength distribution, which will lead to a narrowing of the cone. This fact is illustrated in Fig. 6. When the pathlength distribution broadens, the average distance between the end points of time-reversed paths increases. As evident within the picture treating the time-reversed paths as double slits, this leads to an increased distance and hence a narrowing of the resulting interference pattern. An averaging over all end-to-end distances then leads to a narrowing of the cone shape. This correction has been quantitatively calculated by Zhu, Pine, and Weitz [1991], Lagendijk, Vreeker, and de Vries[1989], who find a strong dependence of the resulting value of kl^* estimated from the full width at half maximum. Instead of FWHM $= 0.75/(kl^*)$ for the scaling of the width as obtained from Eq. 1.3, Zhu, Pine, and Weitz [1991] find a scaling as:

$$FWHM^{-1} = \left(\frac{2}{3} + \frac{2(1+R)}{3(1-R)}\right) kl^*, \tag{2.1}$$

where R is the angular averaged reflectivity due to the index mismatch. Thus the values of kl^* obtained from a fit to Eq. 1.3 need to be corrected by a factor of 1/(1-R). This correction becomes important in the quest for Anderson localization as in that case the particles are very strongly scattering and the samples therefore have relatively high refractive indices. Thus

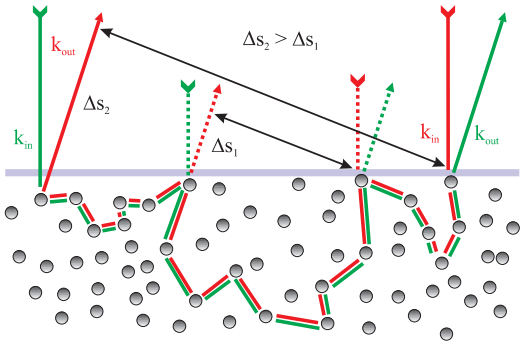

Figure 6: In case the effective refractive index of the scattering medium is high, internal reflections at the sample boundary may occur. These internal reflections in turn lead to an overpopulation of longer end-to-end distances of photon paths. Since the backscattering cone originates from the interference of time-reversed photon paths, this overpopulation then artificially narrows the measured cones, such that the determination of kl^* directly via the width leads to an overestimation of its inherent value.

they show increased internal reflections, which would lead to an overestimation of the value of kl^* solely from the width of the backscattering cone. In order to perform the above correction, the refractive index mismatch at the surface of the sample needs to be known, i.e. the effective refractive index of the sample needs to be calculated. To a first approximation, this can be done following Garnett [1904], but this approach is only strictly valid for particles with a small refractive index. In order to take into account the strong scattering cross-sections of the particles, more elaborate schemes are necessary. Such calculations have been pioneered by Soukoulis and Datta [1994], Busch and Soukoulis [1996].

2.1.4. Recurrent scattering

As the turbidity of the samples increases, there is an increased probability for multiple scattering paths to return upon themselves. In the extreme case, this will lead to Anderson localization, when such paths become macroscopically populated. Wiersma, van Albada, van Tiggelen, and Lagendijk [1995] have studied the backscattering cone for increasingly turbid samples and have found that with decreasing kl^*, the enhancement factor

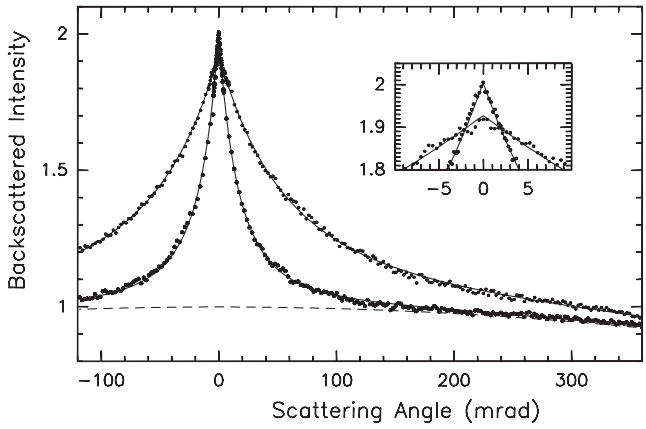

Figure 7: For very turbid samples, the enhancement in the backscattering direction is reduced as can be seen from a close-up at the cone-tip of different samples. This is argued to be due to an underpopulation of time-reversed paths because for very turbid samples, there is an increased probability of visiting the same scatterer twice in a multiple scattering path. Therefore such paths do not contribute fully to the interference pattern resulting in the backscattering cone. Reprinted figure with permission from Wiersma, van Albada, van Tiggelen, and Lagendijk [1995]. Copyright 1995 by the American Physical Society.

of the backscattering cone is reduced. When the first and last scatterer of a multiple scattering path are the same, the contribution of the interference with the time-reversed path will be the same as that of the background. This implies that the background will be overestimated leading to a reduction of the enhancement factor. An illustration of this is shown in Fig. 7 for two different samples with values of kl^* of 22 and 6 respectively. Due to the high resolution and wide angular range of their setup described above (Wiersma, van Albada, and Lagendijk [1995]), the enhancement factor is claimed to be determined to roughly one percent. Thus the reduction shown in Fig. 7 should be significant.

It should be noted however that in these measurements of the backscattering cone, there is no absolute determination of the intensity scale. The level of the incoherent background is simply determined from a cosine shaped fit in addition to the backscattering cone described by Eq. 1.3.

As such, the backscattering cone would violate the conservation of energy, such that in such strongly scattering samples, the absolute intensity needs to be known. This will be discussed in more detail below where the enhancement is determined over the full angular range with an absolute intensity scale. In fact, the incoherent background can differ by a few percent as the turbidity changes. For instance, as the turbidity increases so does the effective size of the sample, such that the albedos of the different samples may no longer be comparable due to losses at the sample boundary. Similarly, the absorption lengths of the different samples will be different, such that the intensity scale may need to be adjusted. This might be the case for the data in Fig. 7, where the broad cone is more consistent with a rounded tip, thus seems to have a somewhat higher absorption than the sample with a perfect twofold enhancement. As it stands, in the absence of an absolute determination of the incoherent background, the enhancement factor cannot be determined with an accuracy of one percent. Thus the observed decrease may not be significant.

2.1.5. Energy conservation

From the discussion so far it would seem that coherent backscattering violates the conservation of energy: In all of the theoretical calculations discussed above (e.g. Akkermans, Wolf, and Maynard [1986], van der Mark, van Albada, and Lagendijk [1988]), the enhancement of the cone is always positive irrespective of angle and polarization channel. Thus for a non-absorbing sample covering an infinite half-space (i.e. with a reflectivity of 1), more intensity would be scattered back from the sample than is incident. Obviously, this cannot be and there has to be a correction to the angular intensity distribution at high angles, which compensates for the enhancement in the backdirection. However, this correction is small and in order to observe this, the incoherent background needs to be determined absolutely. This was not done so far (e.g. Wiersma, van Albada, van Tiggelen, and Lagendijk [1995], Störzer, Gross, Aegerter, and Maret [2006]) and the backscattering cones thus obtained were well described by Eq. 1.3. In Fig. 8, the result of such a correction is shown. Here the incoherent reference was a teflon sample, where the absorption was determined using a time of flight measurement (Fiebig, Aegerter, Bührer, Störzer, Montambaux, Akkermans and Maret [2007]). Also shown in the figure is a corrected theory, taking into account the fact that when the mean free path gets smaller than the wave-length of light, the time-reversed paths start to overlap.

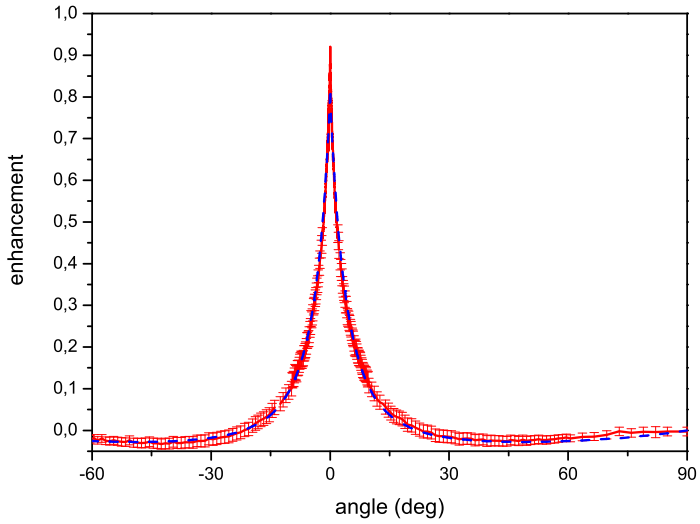

Figure 8: A backscattering cone taking into account the absolute intensity scale. Note that there is a negative contribution at high angles balancing the intensity in the cone. This negative part of the enhancement can be described by a correction based on the finite width of the time-reversed paths. Such a corrected theory is shown by the dashed line. Data from Fiebig, Aegerter, Bührer, Störzer, Montambaux, Akkermans and Maret [2007].

This leads to an underpopulation on these paths and hence a reduction of the backscattering enhancement. This is indicated in the sketch in figure 9, where the overlap of two Gaussian distributed lightpaths is shown. Since this reduction takes place on a length scale of λ, the corresponding reduction of the backscattering enhancement is at high angles. To a first approximation, this correction can be calculated to be (Fiebig, Aegerter, Bührer, Störzer, Montambaux, Akkermans and Maret [2007]):

$$\alpha(q) = \frac{3/7}{(1+ql^*)^2}\left(1+\frac{1-\exp(-4/3ql^*)}{ql}\right)-\frac{9\pi}{7(kl^*)^2}\cdot\left(\frac{\cos\theta}{\cos\theta+1}\right). \quad (2.2)$$

A fit of this equation to the backscattering data with kl^* the only fit parameter can also be seen in Fig. 8, which is in very good agreement with the data. Furthermore, the integrated intensity over the backscattering half-space of this expression (and of the corresponding data) is nearly zero for all values of kl^*, thus showing that including this correction, energy is indeed conserved for coherent backscattering. Such a result can also be obtained from diagrammatic theory (Akkermans and Montambaux [2006]). Here it can be shown that the Hikami-box (Hikami [1981])describing coherent backscattering contains not only the most-crossed diagrams, but also those dressed with an impurity. These diagrams give a contribution of the same order, but negative. It can then be shown exactly that the integral over the whole Hikami-box is exactly zero, which corresponds to the conservation of energy.

2.2. THE INFLUENCE OF A MAGNETIC FIELD

As discussed in detail above, coherent backscattering is fundamentally an interference effect due to the wave nature of light. In order to show this experimentally, one needs to change the phase of the light on counterpropagating paths, such that time-reversal symmetry is broken. A possible mechanism for the breaking of time-reversal symmetry is the application of a magnetic field. As shown by Faraday [1846], an applied magnetic field will change the polarization angle of light passing through a material. This is very pronounced for materials containing paramagnetic rare earth elements, as they possess absorption bands, which lead to a very strong Faraday effect. The magneto-optical rotation of a material is quantified by the Verdet constant, which is the constant of proportionality between the change in phase angle and the applied magnetic field times the length of the light path.

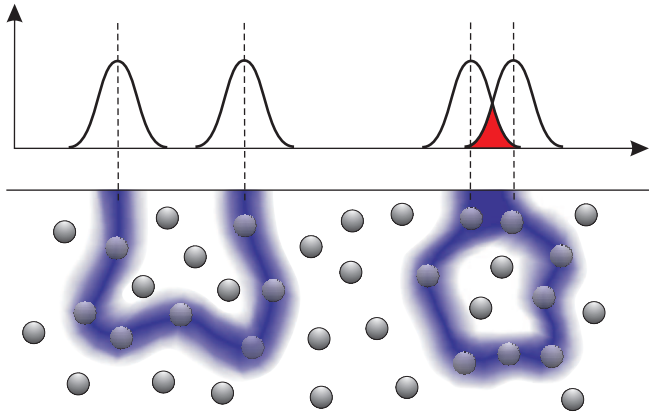

Figure 9: Illustration of the physics behind the reduction of the backscattering enhancement. When the mean free path gets shorter, the end points of the multiple scattering paths start to overlap. Describing these as Gaussian distributions with a width λ, one obtains the correction of Eq. 2.2.

Given the importance of time-reversal symmetry to coherent backscattering and the possibility of influencing the phase of light inside a multiple scattering medium via the Faraday effect, Golubentsev [1984], MacKintosh and John [1988] have theoretically studied the effect of a medium with a high Verdet constant on the coherent backscattering cone. Due to the fact that we are dealing with a multiple scattering medium however, things are not so simple that it suffices to project the multiple scattering path onto the applied field in order to obtain the mean angle of rotation of the phase. In fact, because the multiple scattering leads to a depolarization of the light, the average rotation of the phase will be exactly zero irrespective of the applied field and the path-length through the material. MacKintosh and John [1988] have however shown in a model, where every scattering event is assumed to randomly change the polarization of the light that the mean square displacement of the phase rotation does follow the Faraday effect. They find that

$$\langle \Delta\alpha^2 \rangle = \frac{4}{3} V^2 B^2 s l_f^*, \tag{2.3}$$

where s is the length of the path and l_f^* is a length scale describing the depolarization of the photons. This length scale will be of the order of the

mean free path l^*, but will depend on the depolarization properties (and hence sizes) of the scattering particles. We will discuss a numerical investigation of these issues in more detail below. From this result it can be concluded that on pathlengths exceeding $(l_f^*(2VB)^2)^{-1}$, photons on counterpropagating paths can no longer interfere with each other, such that localization is destroyed.

Other effects of magnetic fields on light transport in random media have been discussed as well, these include the existence of the analogue of the Hall effect for photons (Rikken and van Tiggelen [1996], Sparenberg, Rikken, and van Tiggelen [1997]), as well as that of transverse diffusion of light (van Tiggelen [1995]).

2.2.1. Destruction of the backscattering cone

As discussed above, for sufficiently strong magnetic fields, Verdet constants and pathlengths, the Faraday effect will lead to a suppression of interference of counterpropagating photons. As we have seen above, the cone tip is due to the longest paths, such that to a first approximation, one could describe the cone in the presence of a magnetic field by introducing the length scale $(l_f^*(2VB)^2)^{-1}$ as an absorption length in the expression of the cone. With increasing field, this length scale decreases, such that eventually, the cone should disappear completely. The field strength at which the cone would be reduced to half its size can be estimated by noting that the width corresponds to a length scale of l^*, such that (taking $l_f^* = 2l^*$ for simplicity) $B = 1/Vl^*$. For a molten Faraday active glass, with a Verdet constant of roughly 10^3 1/Tm and a mean free path of roughly 100 μm, one obtains a field of roughly 10 T. A corresponding experiment was carried out by Erbacher, Lenke, and Maret [1993], who studied the field dependence of the backscattering cone in a Faraday active glass powder in fields up to 23 T. As can be seen in Fig. 10, the application of 23 T to the material leads to an almost complete destruction of the backscattering cone in accordance with the theoretical prediction. For the theoretical curves, q^2 was replaced by $q^2 + q_F^2$, where $q_F = 2VB$ describes the depolarization due to the magnetic field.

2.2.2. Polarization effects

The simple helicity-flip model of MacKintosh and John [1988] can well describe the data when the incident light is parallel to the applied field. However, if the field is perpendicular to the illumination, the cone-shape

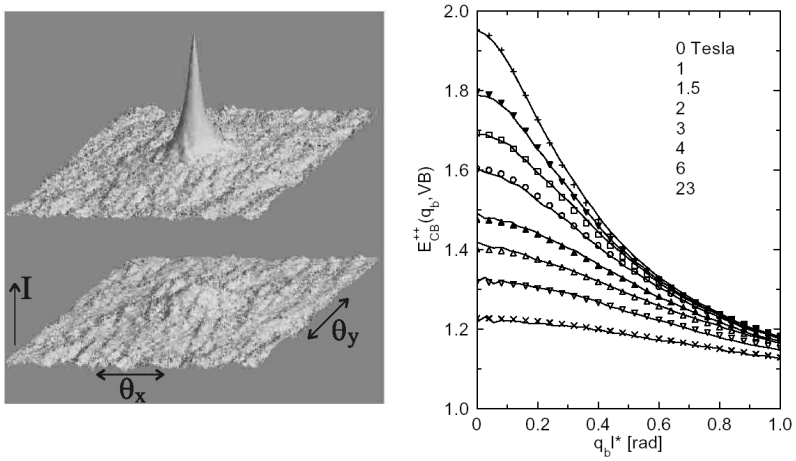

Figure 10: Destruction of the backscattering cone by a magnetic field. The left hand panel illustrates the destruction of the cone in both angular dimensions, whereas the right hand panel describes the reduction of the enhancement as a function of different applied fields. The data are from Lenke and Maret [2000].

can no longer be described by a modified version of Eq. 1.3 as was shown by Lenke, Lehner and Maret [2000]. In fact as can be seen in Fig. 11, the backscattering cone may even split into two peaks, which then diminish in intensity. In order to describe these data, the polarization dependence of the scattering process has to be taken into account, which goes beyond the helicity-flip model and has to be done numerically. Such an investigation was carried out by Lenke and Maret [2000]. In their treatment, Faraday rotation takes place only between scattering events, as is the case in the helicity-flip model of MacKintosh and John [1988], but at each point in a simulation of a random walk, the full scattering matrix of Rayleigh-Debye-Gans theory is applied to the polarization. The result of such a simulation is also shown in the right hand panel of Fig. 11. As can be seen from comparing both parts of the figure, the simulation can qualitatively describe the data. Physically, this splitting of the cone peak is due to the fact that in this transverse setup, there is a net, magnetic field dependent phase change on the time reversed paths given by the end-to-end distance. This phase difference needs to be compensated for by the phase change due to the pathlength difference at different angles. For circular polarization, this leads to a shift of the peak, whereas in linear polarization, the different angular directions are equivalent, such that a splitting of the cone peak is observed (Lenke and Maret [2000]).

This description of magnetic field effects on the backscattering cone are fundamentally determined by the length scale l_f^*, which describes the polarization. For Rayleigh scattering, it can be shown that $l_f^* = 2l^*$ (Lenke and Maret [2000]). However, as the scattering particles increase in size, Mie theory has to be used to describe the polarization effects of each scattering event. This has been studied by Lenke, Eisenmann, Reinke, and Maret [2002] for different sized particles of the order of the wavelength of light, where good agreement is found with the predictions from Mie-theory.

2.3. COLD ATOMS

With the advent of laser-cooling and the corresponding successes in cooling atomic gases to very low temperatures, a new field of the investigation of multiple scattering has been opened. Due to the fact that in a cold cloud of atoms all scatterers are identical, one can exploit the properties of resonant scattering in order to increase the scattering cross-section manyfold. This may in the future allow such a reduction of kl^* for these samples that the Ioffe-Regel criterion is fulfilled and Anderson localization can be observed.

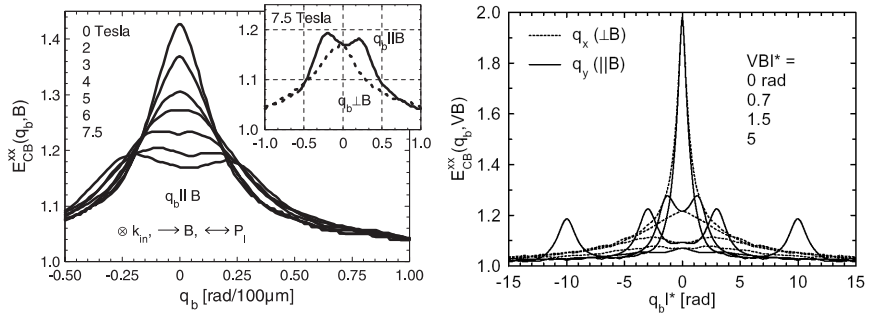

Figure 11: The influence of the field direction and the incident polarization on the backscattering cone in a magnetic field. Experimental data are on the left, simulation results on the right. If the field is not applied parallel to the incident light, the destruction of the cone cannot be described by a modified version of Eq. 1.3. A simulation taking into account the full scattering matrix for all scattering events on a multiple scattering path however can describe the data. Adapted from Lenke and Maret [2000], Lenke, Lehner and Maret [2000].

So far however, only the backscattering cone has been observed and the situation has proven to be somewhat more complicated than hoped at first. This is because of the importance of microscopic degrees of freedom in atomic scattering, which can greatly influence e.g. time-reversal symmetry. This will be discussed in detail below and can lead to the observation that the backscattering cone is not destroyed by the presence of a magnetic field as we have seen above, but rather is recovered due to a magnetic field. At present, investigations of multiple scattering of light in cold atomic gases is limited to Rb and Sr, which show vastly different behaviour due to their different ground state degeneracies.

2.3.1. Rb atoms

Due to the fact that the cooling of Rb atoms is well known and understood, the first backscattering cones from cold atomic gases were scattered by Rb atoms (Labeyrie, de Tomasi, Bernard, Müller, Miniatura and Kaiser [1999], Kupriyanov, Sokolov, Kulatunga, Sukenik, and Havey [2003]). However, as can be seen in Fig. 12, the observed enhancement is only between 1.1 and 1.15, thus much smaller that that observed in colloidal suspensions and

powders. Due to the internal structure of the Rb atoms, especially the fact that the ground state is degenerate, time reversal symmetry is partially broken. This is similar to the Faraday rotation effects discussed above for colloidal powders. The degeneracy of the ground state may lead to a change in helicity of the photon during a scattering event, by changing the ground state of the atom (Jonckheere, Mller, Kaiser, Miniatura, and Delande [2000]). This could be treated by a model similar to the helicity-flip model (MacKintosh and John [1988]) devised to take into account the effect of Faraday rotation inside a material with high Verdet constant. Müller, Jonckheere, Miniatura, and Delande [2001] calculated this explicitly and find good agreement with the experimental reduction of the cone enhancement (Labeyrie, de Tomasi, Bernard, Müller, Miniatura and Kaiser [1999]). They also find that different orders of scattering contribute differently to the effect. In fact, if only double scattering were taken into account, the reduction effect would be much less pronounced with enhancement factors of up to 1.7 being possible (Jonckheere, Mller, Kaiser, Miniatura, and Delande [2000]). By lifting this degeneracy using an applied magnetic field, the enhancement of the backscattering cone could be recovered.

2.3.2. Sr atoms

In order to be able to study a system with a good enhancement factor in the absence of a magnetic field, a cloud of atoms with a non-degenerate ground state had to be used. This is much more difficult as the cooling transitions are harder to excite in this case. However using Sr atoms, it was possible to cool a cloud sufficiently to observe a coherent backscattering cone (Bidel, Klappauf, Bernard, Delande, Labeyrie, Miniatura, Wilkowski, and Kaiser [2002]). The resulting cone is shown in Fig. 13 and has an enhancement factor of nearly two in accord with the expectation. Thus the study of Sr clouds may hold the promise of increased coherence length, such that multiple scattering samples with very long coherent light paths can be studied. This may then lead to the observation of Anderson localization in such samples.

In this context it should be noted however that due to the exploitation of resonance scattering to reduce the mean free path, the propagation speed of photons is slowed down remarkably (Labeyrie, Vaujour, Müller, Delande, Miniatura, Wilkowski and Kaiser [2003]). This means that the increased dwell time in the scattering cavity may also lead to a loss of coherence due to the motion of scatterers on this time scale. This was investigated

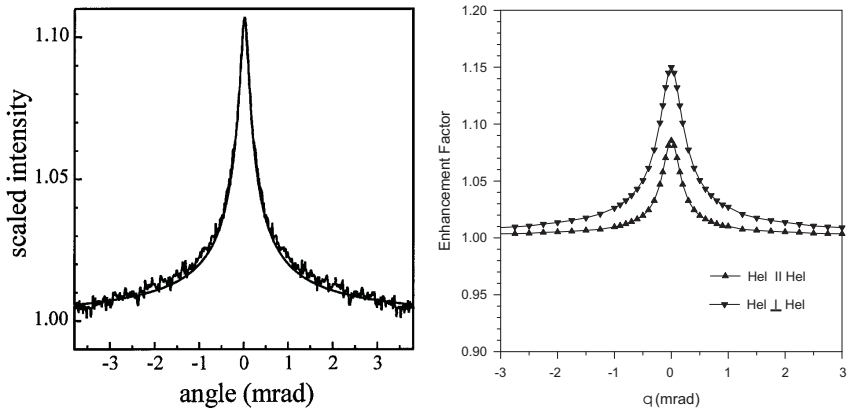

Figure 12: Backscattering cone from a cloud of cold Rb atoms (on the left data from Labeyrie, de Tomasi, Bernard, Müller, Miniatura and Kaiser [1999] are shown, while on the right data from Kupriyanov, Sokolov, Kulatunga, Sukenik, and Havey [2003] are presented). Note that the enhancement factor is very low compared to that seen for colloidal suspensions or powders. This is connected to the internal degrees of freedom of the atoms in question as will be discussed in the text. Reprinted figure with permission from Labeyrie, de Tomasi, Bernard, Müller, Miniatura and Kaiser [1999] and Kupriyanov, Sokolov, Kulatunga, Sukenik, and Havey [2003].

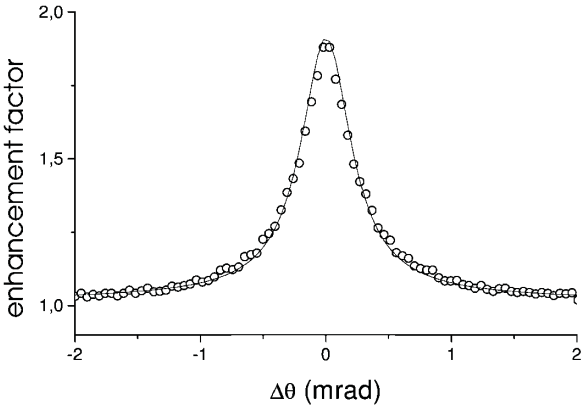

Figure 13: Backscattering cone from a cloud of cold Sr atoms Bidel, Klappauf, Bernard, Delande, Labeyrie, Miniatura, Wilkowski, and Kaiser [2002]. Here, almost perfect enhancment is observed, which is due to the fact that the magnetic moment of Sr does not allow for internal degrees of freedom to be scattered from. Reprinted figure with permission from Bidel, Klappauf, Bernard, Delande, Labeyrie, Miniatura, Wilkowski, and Kaiser [2002]. Copyright 2002 by the American Physical Society.

using Monte Carlo simulations (Labeyrie, Delande, Müller, Miniatura and Kaiser [2003]), where it was shown that only a few scattering events are taking place with coherent light, such that the long multiple scattering paths necessary for Anderson localization to occur are out of reach. We will get back to the point of reduced transport velocity due to resonant scattering in the discussion of colloidal powders below.

2.4. OTHER TYPES OF WAVES

In addition to localization of light waves and electronic waves, localization was searched for in many other types of waves. Given the difficulties faced by electron-localization due to the presence of interactions, these studies have focused on non-interacting waves, such as acoustic, seismic and matter waves. Due to the fact that in these waves strong scattering cross-sections however are difficult to obtain, most of these studies have concentrated on the observation of weak localization.

2.4.1. Seismic waves

Multiple scattering of seismic waves has recently become a very interesting subject, leading for instance to an increased precision in the determination of the earth's structure from the noise in seismographs (Snieder, Grêt, Douma, and Scales [2002], Campillo and Paul [2003], Shapiro, Campillo, Stehly, and Ritzwoller [2005]). In the context of interest here, Larose, Margerin, van Tiggelen, and Campillo [2004] have studied the reflection of a stimulus from a sledge hammer that was repeated fifty times for each measurement as a function of distance from the source. The results are shown in Fig. 14. The different lines correspond to different delay times between the stimulus and the reflected signal. As expected from the theoretical description above, the backscattering cone arises from long multiple scattering paths, such that the signal only appears at long delay times. Particulary as can be seen from the figure, an enhancement factor of two can be observed from the long paths observed at late times.

In order to be able to observe this enhancement, i.e. to suppress any incoherent background, the experiment was carried out at night in a sparsely populated region as well as under anticyclonic conditions.

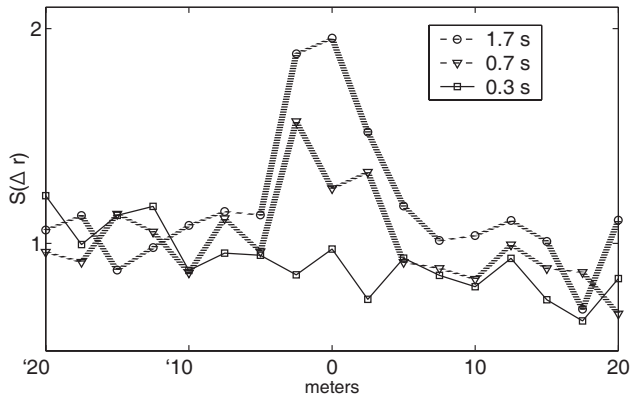

Figure 14: Backscattering cone of seismic waves produced by Larose, Margerin, van Tiggelen, and Campillo [2004]. The different lines show the signal of buried seismogrphs at a certain distance from the stimulus as a function of delay time. After long times, the multiply scattered paths in the backdirection show a coherent backscattering cone with an enhancement factor of nearly two. Reprinted figure with permission from Larose, Margerin, van Tiggelen, and Campillo [2004]. Copyright 2004 by the American Physical Society.

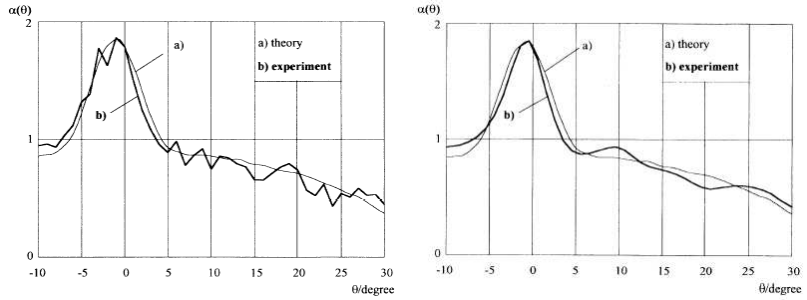

Figure 15: Backscattering cone of ultrasonic waves through gravel stones (left) and brass rods (right). These data were obtained by Bayer and Niederdränk [1993]. The thin lines show the theoretical expectation (Kirkpatrick [1985]), whereas the thick lines show the experimental results. The data correspond to signals at a certain time delay, similar to those of the seismic waves in Fig. 14 of 22 μs and 40 μs respectively. Reprinted figure with permission from Bayer and Niederdränk [1993]. Copyright 1993 by the American Physical Society.

2.4.2. Acoustic waves

Well before the study of seismic waves propagating in disordered media, the behaviour of multiple scattered ultrasonic waves in the MHz range was investigated. Here, Kirkpatrick [1985] has theoretically calculated the properties of localized waves in a random medium and Bayer and Niederdränk [1993] have experimentally studied the backscattering cone from e.g. gravel using ultrasonic waves. This was done in both two and three dimensional systems and good agreement with theory was found, as illustrated in Fig. 15.

More recently, there have been experiments studying time resolved transmission of acoustic waves through samples of aluminium beads by Page [2007]. In these experiments, a non-exponential decay of the time-resolved transmission was found. As will be discussed below in the context of light, this is a strong indication of non-classical transport and localization. In addition, the statistics of speckles was studied for these samples, where again strong deviations from the behaviour diffuse waves were found (**?**).

2.4.3. Matter-waves

There are two different types of matter waves, where efforts are under way to localize them. In the first instance, the advent of laser cooling and optical traps has lead to the proposal of studying Anderson localization of cold atoms in disordered optical traps. These optical traps are usually provided by a speckles pattern from a laser source passed through a disordered medium. It has been found however that in that case, the average spacing of the speckle spots is difficult to reduce to the scale that the Ioffe-Regel criterion can be reached (Lye, Fallani, Modugno, Wiersma, Fort, and Inguscio [2005], Clément, Varón, Hugbart, Retter, Bouyer, Sanchez-Palencia, Gangardt, Shlyapnikov, and Aspect [2005], Kuhn, Miniatura, Delande, Sigwarth, and Müller [2005]). In addition, dense clouds of cold atoms are troubled by strong interactions, such that a Mott insulator can be observed, but Anderson localization is still out of reach in present experiments. In fact, there is no observation of a backscattering cone of cold atoms in disordered optical lattices to date.

A second type of proposal is to localize ultracold neutrons in the presence of disorder (Igarashi [1987]). Here, progress has been made in cooling the neutrons sufficiently to be able to observe their multiple scattering. The angular resolution of neutron detectors is however not sufficient at present to observe the corresponding, narrow backscattering cone (Stellmach, Abele, Boucher, Dubbers, Schmidt and Geltenbort [2000], Stellmach [1998]).

§ 3. The transition to strong localization

In the above experiments, the critical parameter for localization, the disorder as measured by $(kl^*)^{-1}$ was small compared to one. The effects of weak localization could however still be observed as there is a counterpropagating path to every path in the backdirection. In order to see effects of strong localization, one needs to strongly increase the probability of the formation of closed loops, such that the renormalization discussed in the theory part can become important. This can be done in principle via an increase in the disorder in order to reach the limit proposed by Ioffe and Regel [1960]. In practice however, this turns out to be difficult as one needs to have strongly scattering samples with low absorption, two conditions which are usually mutually exclusive. However making use of the properties of Mie-resonances in the scattering cross-section (Mie [1908]), this is possible as we will see below. On the other hand, spatially restricting the propagation will lead to a strong increase in the probability of observing crossings of the paths. This is exploited in the study of quasi-one dimensional systems where localization of microwaves has been observed (see e.g. Chabanov, Stoytchev, and Genack [2000]).

3.1. LOW DIMENSIONAL SYSTEMS

In low dimensional systems, one has several advantages to study localization. First of all, scaling theory predicts that in less than two dimensions, localization will always be present (Abrahams, Anderson, Licciardello, and Ramakrishnan [1979]). The occurrence of localization will in this case go together with the increase in system size and localization effects can be observed for large enough samples. The spatial restriction in quasi-one-dimensional samples leads to a natural reduction of the dimensionless conductance thus leading to a presence of localization even far above the turbidity demanded by Ioffe and Regel [1960]. This, in turn, also implies that the transition to localization cannot be studied in low dimensional systems, and for a proper study of the scaling theory of localization, three dimensional studies are needed.

The most successful experimental low dimensional system so far constitutes a quasi-one dimensional case, where alumina spheres of a diameter of roughly a centimeter are placed inside a copper tube of a diameter of 7 cm and a length of roughly one meter (Chabanov and Genack [2001]). The alumina particles then scatter microwaves, which are contained in the

copper tube as in a wave guide, thus producing the quasi-one dimensional character of the system.

3.1.1. Statistical features

The transmitted microwave intensity through the cavity shows strong fluctuations as a function of input frequency (see Fig. 16 a) Such fluctuations always arise in the case of a multiple scattering sample. They arise from interferences of the randomly distributed field and are known as speckle. Due to the fact that speckles originates from a random distributions of fields it is easy to show that a diffusive speckle shows an exponential intensity distribution. As can be seen in Fig. 16 b, in the case of a quasi-one dimensional sample longer than the localization length, the intensity distribution of the fluctuations is much wider than the exponential distribution expected for a diffusive speckle indicated by the dashed line (Chabanov, Stoytchev, and Genack [2000]). The intensity distribution is rather given by a stretched exponential with an exponent of 1/3 (Chabanov, Zhang, and Genack [2003]), in agreement with the prediction of Kogan, Kaveh, Baumgartner, and Berkovits [1993], whereas Nieuwenhuizen and van Rossum [1995] have predicted a stretched exponential with an exponent of 1/2. This result was later confirmed by Kogan and Kaveh [1995].

The advantage of studying the fluctuations of the intensity rather than the static intensity is that this measure is not affected by the presence of absorption. As we will see below in the discussion of static transmission measurements in three dimensional samples, the presence of absorption can be a great problem in the identification of localization from transmission measurements alone. In addition to the probability distribution of the speckle intensities, Sebbah, Hu, Klosner, and Genack [2006] have measured the spatial distribution of the localized modes.

3.1.2. The path length distribution

Another strategy of avoiding problems with absorption influencing the interpretation of experimental results is to study time-resolved transmission. This will be discussed in more detail below in the context of three dimensional systems, but time resolved measurements were also carried out in the quasi-one dimensional system described above by Chabanov and Genack [2001]. The results of such measurements for four different samples are shown in Fig. 17. The different samples differ in tube length, ranging from 61 (sample A) to 183 cm (sample C). Samples B and D are both 90 cm long

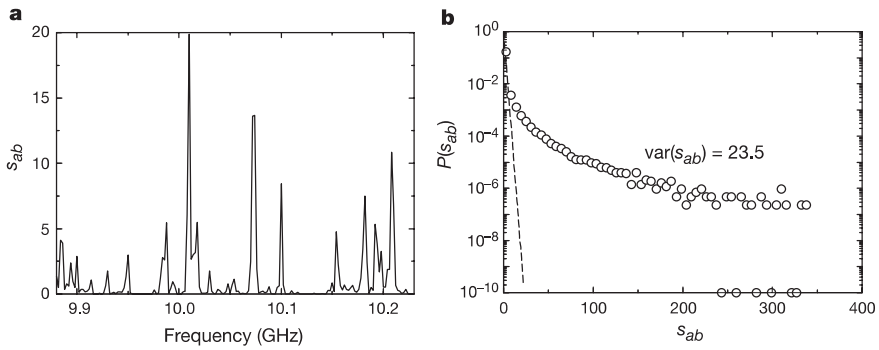

Figure 16: Measurements of the fluctuations of photons in a quasi-one dimensional sample of alumina spheres obtained by Chabanov, Zhang, and Genack [2003]. Part a) shows the intensity as a function of input frequency for a certain realization of the disorder in the tube. Averaging over many realizations of the disorder, the intensity probability distribution in part b) is obtained. This shows clear deviations from the classical exponential distribution and rather shows a stretched exponential with an exponent of 1/3 (Chabanov, Zhang, and Genack [2003]). Reprinted figure with permission from Chabanov, Zhang, and Genack [2003]. Copyright 2001 by the American Physical Society.

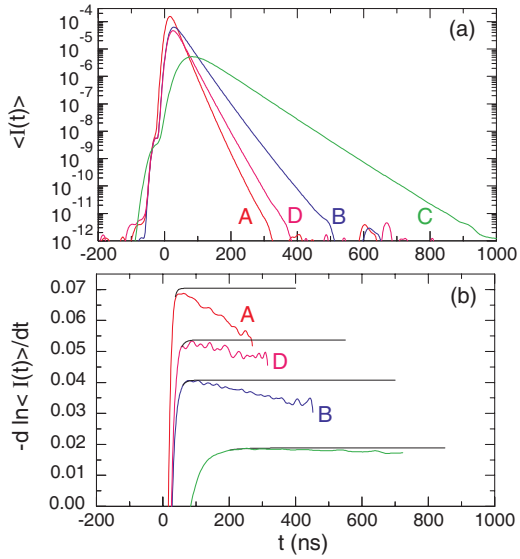

Figure 17: Measurements of the pathlength distribution of photons in a quasi-one dimensional sample of alumina spheres of different lengths as obtained by Chabanov and Genack [2001]. As can be seen from the lower part of the figure, the diffusion coefficient in these samples shows a time dependence indicating a breakdown of diffusion due to the presence of pre-localized states. Reprinted figure with permission from Chabanov and Genack [2001]. Copyright 2001 by the American Physical Society.

but sample D has artificially enhanced absorption by adding a titanium foil to the tube.

The data in Fig. 17 are shown on a semi-logarithmic scale and show a slight deviation from the purely exponential decease at long times expected from diffusion. This is shown with more clarity in the lower part of the figure, where the derivative of the logarithm of the intensity with respect to time is shown. At long times, this should be a constant given by a combination of the absorption length and the diffusion coefficient. As can be seen, there is a decrease in the diffusion coefficient with time, which is most prominent for sample A. In addition, comparing samples B and D shows that indeed the change in absorption only leads to a constant

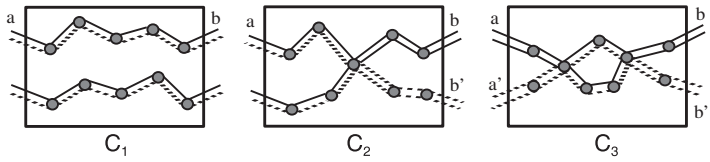

Figure 18: The nuber of diffusive modes is inverse to the probability of crossings of paths inside the sample adapted from Scheffold and Maret [1998]. For very constrained samples, such as in the case of the quasi-one dimensional microwave experiments or the measurements on universal conductance fluctuations, the probability of crossings is high and thus the number of modes, i.e. the control parameter for localization, is low. Reprinted figure with permission from Scheffold and Maret [1998]. Copyright 1999 by the American Physical Society.

shift in the decay rate and thus does not influence the results of the time dependence shown in the figure.

In contrast to the results in three dimensions discussed below, the diffusion coefficient here decreases linearly with time. Such a decrease is obtained from weak localization corrections in the quasi-one dimensional case as discussed by Cheung, Zhang, Zhang, Chabanov, and Genack [2004] and Skipetrov and van Tiggelen [2004].

3.1.3. The connection to bulk experiments

As was mentioned above, experiments in such quasi-one dimensional systems exploit the increased probability of paths crossing due to the constricted geometry. As a matter of fact, a similar approach was used by Scheffold, Härtl, Maret, and Matijević [1997], Scheffold and Maret [1998] to study the universal conductance fluctuations of light which are suppressed by a factor of $1/g^2$ compared to the usual fluctuations. These experiments were carried out in a colloidal suspension of TiO_2 particles with values of kl^* of the order of 20. This shows that a geometric confinement gives rise to mesoscopic effects, which are similar to the bulk effects of Anderson localization in that they depend on interference between different paths, however they are solely due to geometric effects and thus should not be confused with bulk Anderson localization.

In fact when estimating the dimensionless conductance (Scheffold and Maret [1998]) for a true bulk sample with dimensions of roughly 10^4 l^*,

one finds that g is very large. For the samples with very low values of kl^* discussed below, one obtains $g \sim 10^4$ (Aegerter, Störzer, Fiebig, Bührer, and Maret [2007]). This demonstrates that in bulk samples, the critical parameter is indeed kl^* as opposed to g and one cannot think of the problem in terms of separated modes. This difference also clearly shows up in the selfconsistent theory of Skipetrov and van Tiggelen [2004] adjusted for finite systems. In the quasi-one dimensional case (Skipetrov and van Tiggelen [2004]), there are pre-localized states and a crossover to localization whereas in the three-dimensional version of the theory (Skipetrov and van Tiggelen [2006]), there are no pre-localized states and diffusion only breaks down at later times.

3.2. STATIC MEASUREMENTS

Static measurements have the strong advantage experimentally of being reasonably simple in their setup. However, in terms of an observation of localization, there is a great problem with most static measurements insofar that a photon which is lost due to absorption cannot be distinguished from one which is lost due to localization. Thus, pure measurements of numbers of photons either in transmission or reflection are difficult to interpret in the context of localization. One way around this is discussed in the end of this chapter and consists of studying the fluctuations of the static intensity (i.e. the speckle). There, the interference terms are of great importance, such that one does not simply look at numbers of photons, such that the different nature of localization and absorption can be distinguished (Chabanov, Stoytchev, and Genack [2000]). Another possibility is offered by time-resolved measurements, which will be discussed in the next section.

3.2.1. Decrease in transmission

As discussed above, localization will lead to a strong decrease in the transmission of photons through the sample. In fact, due to the renormalization of the diffusion coefficient, the dependence of the transmission on the sample thickness can be predicted. In the critical regime, where there is no length scale in the diffusion left, scaling theory predicts the diffusion coefficient to decrease as $1/L$ (Abrahams, Anderson, Licciardello, and Ramakrishnan [1979]). This leads to a decrease in transmission proportional to $1/L^2$ (Anderson [1985], John [1984]). Deep in the localized regime, where the diffusion coefficient vanishes, the transmission will be suppressed exponentially, as only the tails of the probability distribution

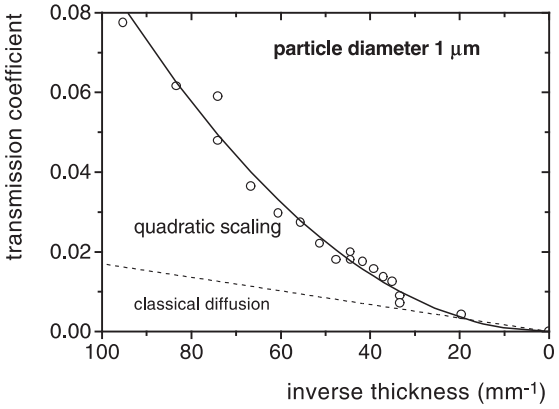

Figure 19: Static transmission through samples of GaAs of average particle size of roughly 1 μm (Wiersma, Bartolini, Lagendijk, and Righini [1997]). As can be seen, the thickness dependence of the transmission does not follow a $1/L$ dependence. However, the dashed line in the figure indicating classical diffusion is inconsistent with a physical interpretation of the data. Any physical effect, be it localization or absorption would lead to a decreased transmission as compared to the classical expectation, whereas the dashed line in fact indicates an *increased* transmission with respect to the diffusive expectation. This is most probably due to the fact that the value of kl^* is underestimated due to the neglecting of absorption in the sample (see text and Fig. 20).

are capable of leaving the sample at the boundary (Anderson [1985], John [1984]). These predictions have been the basis of an experimental search for localization using static transmission measurements of strongly scattering samples (Wiersma, Bartolini, Lagendijk, and Righini [1997]). In this work, the transmission properties of ground samples of GaAs were studied in the near infrared, at a wavelength of 1064 nm. For different degrees of grounding and hence different average particle sizes, marked differences in the thickness dependence of transmission was observed. The scattering properties of the samples were characterized using the initial slope of the coherent backscattering cone, yielding a value of kl^*.

The results for a sample consisting of particles of an average diameter of 1 μm are reproduced in Fig. 19. As can be seen in the figure, there are deviations from the expected $1/L$ behaviour corresponding to diffusion.

The theoretical prediction shown by the dashed line however is in strong contradiction with a simple understanding of localization. As it is shown in the figure, the deviations from classical transmission due to localization lead to an *increase* in static transmission, which is physically impossible. Moreover, the deviations increase with decreasing sample thickness again in contradiction with a physical understanding of the situation. The theoretical prediction of classical diffusion was obtained from the measurement of kl^* due to the initial slope of the backscattering cone. This yields a mean free path of 0.17 μm and a corresponding value of $kl^* = 1$. The transmission measurements from thin samples are however more consistent with a value of $kl^* \simeq 5$. In this case the deviations in thicker samples are such that the number of transmitted photons decreases compared to the classical expectation. This implies that the determination of kl^* from the initial slope of the backscattering cone is systematically flawed and underestimates the value of kl^*. As we have seen above, absorption can lead to a rounding of the cone tip. Such a rounding strongly influences the initial slope of the cone, while leaving the width more or less unchanged. Thus the presence of absorption may very well lead to an underestimation of kl^* from the initial slope of the backscattering cone, whereas an estimate from the width of the cone is less susceptible to absorption. This is corroborated by the fact that the value of kl^* estimated above is in good agreement with a reanalysis of the cone shape using the width of the cone to determine kl^* and including absorption, shown in Fig. 20 (Scheffold, Lenke, Tweer, and Maret [1999]).

This reanalysis also leads to an estimation of the absorption length of $L_a \simeq 8$ μm, which is consistent with the transmission data, again shown in Fig. 20. This means that the deviations from diffusive behaviour are most probably due to an increased absorption induced by the longer grinding. Such absorption may for instance be due to the increased appearance of surface states.

For even smaller particle sizes (average diameter 300 nm), Wiersma, Bartolini, Lagendijk, and Righini [1997] even obtain an exponential decrease of transmission with a typical length scale of $L \simeq 5$ μm. Supposing that with decreasing particle size the mean free path also decreases and the absence of absorption, this would be in accord with the prediction of Anderson localization in the localized regime (Anderson [1985], John [1984]). Unfortunately however, the scattering properties of this sample are not characterized by any measurement, such that we do not know what the value of kl^* of this sample should be. This also makes it impossible to

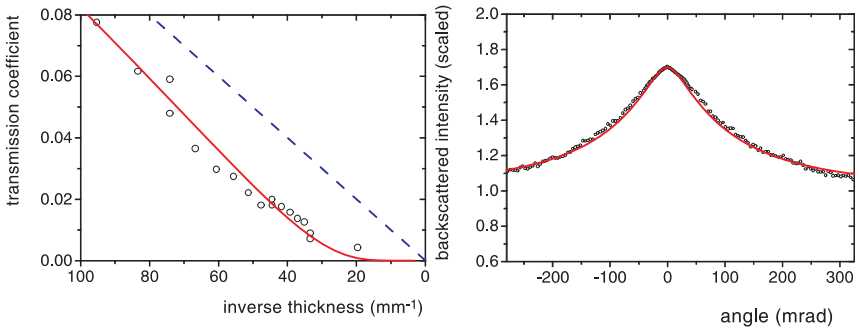

Figure 20: The data of Wiersma, Bartolini, Lagendijk, and Righini [1997] (see Fig. 19) as reanalysed by Scheffold, Lenke, Tweer, and Maret [1999]. In this analysis, the infuence of absorption has been taken into account as well. Thus, the tip of the cone is rounded and the slope at that point cannot be used for a reliable estimate of kl^*. The analysis of the cone shape (right hand side) yields a value of $kl^* \simeq 5$ and an absorption length of $L_a \simeq 8\mu$m, which fits the data very well. Using these parameters, the static transmission measurements on the left hand side can be described without additional parameters. Including absorption, the full red line is obtained, whereas the classical expectation is given by the dashed blue line. Note that in contrast to Fig. 19, the expectation for pure diffusion is above the data, as it should be.

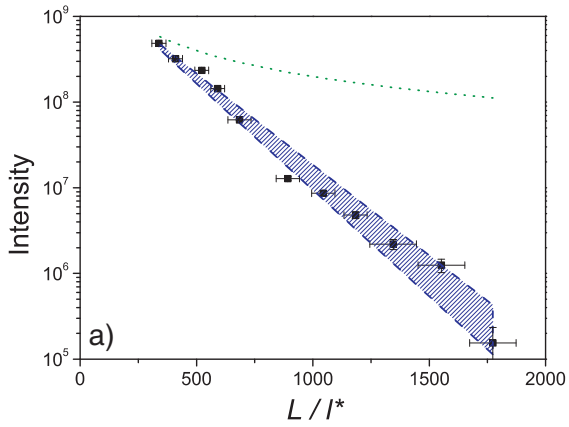

Figure 21: Even for a classical sample (with $kl^* \simeq 20$) that appears white and which does not show significant rounding of the backscattering cone, absorption may be high enough to produce an exponential decrease in transmitted intensity, which appears incompatible with classical diffusion of light (dotted green line) Aegerter, Störzer, Fiebig, Bührer, and Maret [2007]. When determining the absorption length using time-resolved measurements (see below), the resulting exponential decrease (dashed blue line) fits very well with the static measurements.

estimate the absorption length of this sample. Based on the above arguments, absorption will be present also in this sample and the corresponding absorption length would not be inconsistent with the length scale of the exponential decrease in transmission. Furthermore, the decrease in kl^* with particle size is certainly not linear and will certainly show a minimum as the scattering cross-section decreases when the particle size is much smaller than the wavelength of light. Therefore it is questionable that the scattering strength of this sample will be strong enough to be beyond the Ioffe-Regel criterion. In addition, in the absence of an independent determination of the absorption length, an exponential decrease of transmission cannot be claimed to be due to localization as absorption is a much more likely candidate.

This is illustrated in Fig. 21, where the static transmission through a sample with $kl^* \simeq 20$ is shown (Aegerter, Störzer, Fiebig, Bührer, and Maret [2007]). For very thick samples, absorption will always dominate and a simple comparison with the expectation from diffusion (dotted line) will always overestimate the transmission. However in this case, the absorption length was directly determined as well using time resolved measurements (see below). Adding this to the description, the dashed line is obtained which perfectly describes the data without a single adjustable parameter. Here the shaded area between the dashed lines indicates the error bar in the experimental determination of the absorption length.

For samples with much lower values of $kl^* \simeq 2.5$, which also show effects of localization in time-resolved measurements (i.e. a spatially dependent diffusion coefficient, see below) the situation is markedly different (Aegerter, Störzer, and Maret [2006]). This is shown in Fig. 22. Again the dotted line corresponds to diffusion in the absence of absorption which strongly overestimates the transmission through the samples. However, also the description including the experimentally determined absorption (dashed blue line) is in contradiction with the data. Thus in this case the reduced transmission is most probably due to localization of photons. This conclusion is strongly supported by the fact that the time-resolved measurements also allow a determination of the localization length (se below). When including this in the description of the transmission measurements, the full red line is obtained, which describes the data perfectly over twelve orders of magnitude and without any adjustable parameter.

This shows that in static transmission measurements, the problem of absorption may be circumvented by an independent determination of the

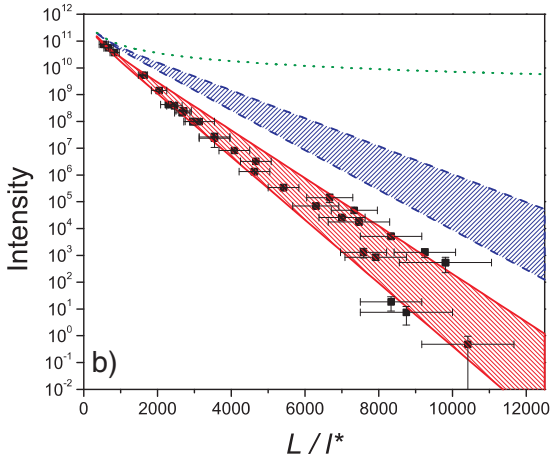

Figure 22: Static transmission measurements through a localizing sample as shown by a long-time tail in time resolved transmission Aegerter, Störzer, and Maret [2006]. As will be shown below, in this case it is possible to not only determine the absorption length, but also the localization length. Again, the green dotted line represents the expectation from pure diffusion and the dashed blue line that of diffusion including absorption. Both curves are incompatible with the measurements and only incorporating the experimentally determined localization length a description of the data becomes possible. In fact there is good agreement between theory and experiment over twelve orders of magnitude without any adjustable parameters.

absorption length. This is most conveniently done in time resolved measurements as we will discuss below.

3.2.2. Influence on the cone-shape

As discussed above, the renormalization of the diffusion coefficient arising from localization can also be treated as a path length dependence of D (van Tiggelen, Lagendijk, and Wiersma [2000]). Since the tip of backscattering cone consists mostly of photons from long paths, such a path length dependence of the diffusion coefficient should also be visible in the tip of the cone in a decrease of the slope as the tip is approached. This effect has been calculated in the framework of self-consistent theory explicitly by van Tiggelen, Lagendijk, and Wiersma [2000]. Their main result is shown in Fig. 23, where the decrease of the diffusion coefficient inside the sample is shown together with the corresponding rounding of the cone-tip. As discussed above however, also absorption leads to a rounding of the cone at small angles due to the lack of photons coming from very long paths. Unfortunately, van Tiggelen, Lagendijk, and Wiersma [2000] obtain a diffusion coefficient which decreases exponentially with sample thickness (analogous to the exponentially decreasing transmission), such that the effect of localization again has the same shape as that of absorption. This means that as in the case of static transmission measurements discussed above, measurements of cone-rounding can only be used as arguments for the observation of localization in the presence of data on the absorption properties of the samples.

Indeed, as a function of sample thickness, Schuurmans, Megens, Vanmaekelbergh, and Lagendijk [1999] find an increasing rounding of the cone when the thickness is decreased as demanded by theory (van der Mark, van Albada, and Lagendijk [1988]). Samples with reasonably high kl^* (shown as full triangles and open squares in Fig. 24) are well described by the linear increase of the cone rounding with $1/kL$. For samples with smaller values of kl^* however, there are marked deviations for thicker samples. In order to determine the influence of absorption, Schuurmans, Megens, Vanmaekelbergh, and Lagendijk [1999] have filled the photoanodically etched GaAs sample showing increased cone-rounding (see figure 5) with dodecanol. This leads to an increase in kl^* as can be seen from a decrease in the width of the backscattering cone (see Fig. 25). Hence the absorption length is also increased according to $L_a \propto \sqrt{l^* l_a}$. A description of the dependence of the cone-rounding on sample thickness of the non-filled sample

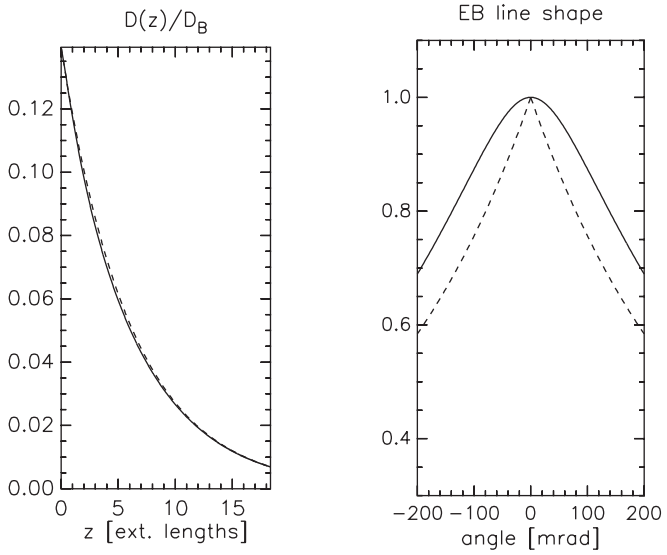

Figure 23: The influence of localization on the tip of the backscattering cone. Due to the fact that photons on long paths are localized and therefore do no longer contribute to the backscattered light, the cone-shape is rounded close to the backscattering directon. Plotted here are results from a self-consistent theory assuming a spatially dependent diffusion coefficient calculated by van Tiggelen, Lagendijk, and Wiersma [2000]. On the left, the spatial dependence of the diffusion coefficient is shown, while on the right the corresponding tip of the backscattering cone is given. The dashed line on the right is the classical cone shape in the absence of localization effects. Reprinted figure with permission from van Tiggelen, Lagendijk, and Wiersma [2000]. Copyright 2000 by the American Physical Society.

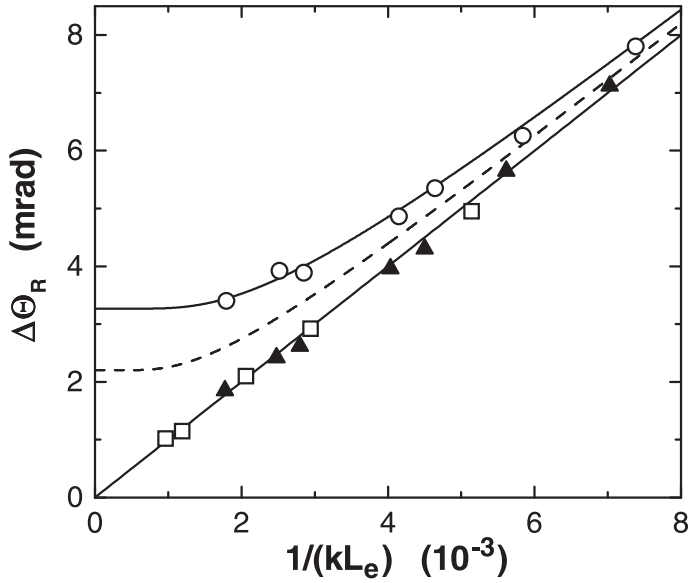

Figure 24: The rounding of the cone shown in figure 5 as a function of sample thickness for different samples Schuurmans, Megens, Vanmaekelbergh, and Lagendijk [1999]. For low values of kl^* (open circles), there are deviations from the expectation of a finite sample. This is in contrast to samples with a higher kl^* (filled triangles and open squares). The open squares are from a similar sample as the open circle, where the pores have been filled with dodecanol. The solid line is a description of the data with absorption. Assuming an unchanged absorption with pore-filling, the dashed line should then correspond to the open squares. Reprinted figure with permission from Schuurmans, Megens, Vanmaekelbergh, and Lagendijk [1999].

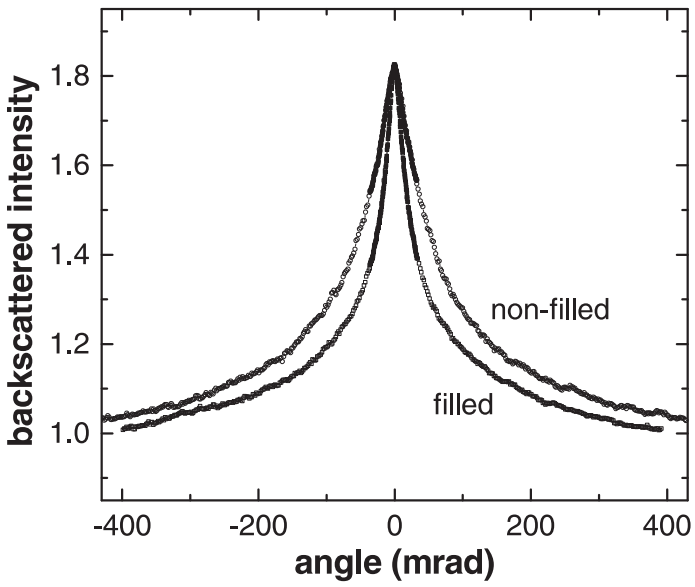

Figure 25: The backscattering cones for photoanodically etched GaP both as produced and filled with dodecanol Schuurmans, Megens, Vanmaekelbergh, and Lagendijk [1999]. As can be seen, the cone of the filled material is narrower indicating an increase in kl^*. Figure 24 has shown that for the filled samples, significantly less cone-rounding has been observed. Reprinted figure with permission from Schuurmans, Megens, Vanmaekelbergh, and Lagendijk [1999]. Copyright 1999 by the American Physical Society.

due to absorption (shown in figure 24 as a dashed line) is not compatible with the thickness dependence of the cone rounding of the filled sample. However, one has to note that in this calculation, Schuurmans, Megens, Vanmaekelbergh, and Lagendijk [1999] have not taken into account the narrowing of the cone due to internal reflections. The filling of the etched holes will lead to a change in the effective refractive index and hence to a change in the value of kl^* determined from the cone width. Thus the filling of the voids may well lead to a decrease in the refractive index and hence to an underestimation in the increase in kl^*. Due to these uncertainties a direct determination of the absorption length in the low-kl^* samples would have been very useful in order to check whether effects of absorption can be ruled out. In addition, subsequent time-resolved experiments on the same samples by Rivas, Sprik, Lagendijk, Noordam, and Rella [2000] and Johnson, Imhof, Bret, Rivas, and Lagendijk [2003] did not show effects of localization in the time domain. While this could be due to the fact that the time-resolved measurements were done on thinner samples (see also below), we note that the transmission data of Johnson, Imhof, Bret, Rivas, and Lagendijk [2003] can be described with an absorption length corresponding to the full line in Fig. 24. It therefore seems that the increased cone rounding observed in these samples cannot be used as an indication of the onset of Anderson localization as long as absorption is not quantified.

3.2.3. Transport speed

Another quantity which can be determined from static measurements is the transport speed of photons in multiple scattering. Since the strong scatterers, which are employed in the search for Anderson localization are roughly of the same size as the wavelength to increase the scattering cross-section, these particles also show resonant scattering (Wigner [1955]). This was first discussed in the context of multiple scattering by van Albada, van Tiggelen, Lagendijk, and Tip [1991]. Contrary to what might be thought intuitively, the resonant scattering properties are still present after averaging over the random distribution of scatterers in the multiple scattering. This leads to a strong decrease in the transport speed of photons. This can be seen in Fig. 26, where the speed of light is shown as a function of particle size. These results were obtained from a calculation using the properties of TiO_2 with a filling fraction of 36%. This has shown that earlier measurements of anomalously low values of the diffusion coefficient in samples of TiO_2 by Drake and Genack [1989] were most probably due to resonant scattering,

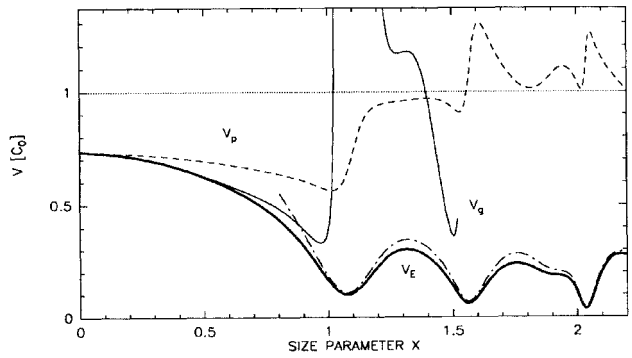

Figure 26: Calculation of the transport velocity as a function of the size parameter van Albada, van Tiggelen, Lagendijk, and Tip [1991]. The calculations were done for particles with a refractive index of 2.72, corresponding to that of TiO_2 in the rutile structure and for a filling fraction of 36 %. Due to the fact that correlations between different scatterers are not taken into account in the calculation, the theory does not fully apply at high filling fractions. Reprinted figure with permission from van Albada, van Tiggelen, Lagendijk, and Tip [1991]. Copyright 1991 by the American Physical Society.

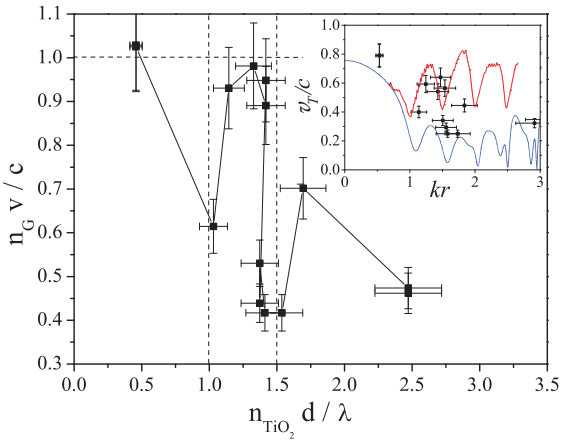

Figure 27: The transport velocity as measured from a combination of time-of flight and backscattering measurements as obtained by Störzer, Aegerter, and Maret [2006]. The main figure shows the velocity relative to its expectation using the Garnett approach. This strongly overestimates the transport speed at particle sizes corresponding to integers of half the wavelength inside the scatterer. The inset shows the transport speed as a function of size parameter compared to theoretical expectations such as that shown in Fig. 26 (blue line). Calculations based on the model of Busch and Soukoulis [1996] that takes into account correlations between scatterers and thus should be applicable for high filling fractions are shown in the red line. Reprinted figure with permission from Störzer, Aegerter, and Maret [2006]. Copyright 2006 by the American Physical Society.

reducing the transport speed and hence the diffusion coefficient, and not the onset of Anderson localization. Subsequently, these calculations were improved by Busch and Soukoulis [1996] and Soukoulis and Datta [1994] to also be valid for higher filling fractions more appropriate to describe experiments. Using a combination of time-resolved transmission measurements (see below) and coherent backscattering measurements, Störzer, Aegerter, and Maret [2006] have measured the transport speed directly for a number of samples with different sizes. These measurements clearly show resonant reductions in the transport speed. The results are shown in Fig. 27 and compared with the theoretical descriptions in the inset (red line Soukoulis and Datta [1994], blue line van Albada, van Tiggelen, Lagendijk, and Tip

[1991]). There is reasonable agreement with the appropriate theory for higher filling fractions. In addition, these measurements show that the reduction in transport speed can be well separated from signatures of localization. Some of the samples studied here do show a non-exponential tail in the time resolved transmission intensity as discussed below. However, these samples do not necessarily show a decrease in transport speed. This is because the Mie-resonances responsible for the increase in scattering cross-section (Mie [1908]) as well as resonant scattering are complemented by resonances in the structure factor, which influences only the scattering cross-section. Thus a suitable particle size and packing fraction can lead to a separation of the effects of localization and resonance scattering (Störzer, Aegerter, and Maret [2006]).

In addition, resonant scattering was also observed in multiple scattering measurements on cold atoms (Labeyrie, Vaujour, Müller, Delande, Miniatura, Wilkowski and Kaiser [2003]), where a decrease in transport speed up to a factor of many orders of magnitude has been observed.

3.2.4. Statistical features

As was discussed in the context of microwave experiments, the statistics of transmitted or reflected photons can also give valuable information about the samples and their possible localization properties. Due to its wave-nature, multiply scattered light shows a characteristic interference pattern known as a speckle. The intensity of each speckle spot will be determined by the differing phase lag between photon paths. For a diffusive sample, the phase delay at different point will be given by a Gaussian distribution, such that the corresponding intensity distribution is given by an exponential. This intensity distribution of the speckle pattern has been characterized by Wolf, Maret, Akkermans and Maynard [1988], where good agreement with the exponential decay of the probability has been found. Vellekoop, Lodahl, and Lagendijk [2005] have recently measured the phase delay directly using interferometric methods (see Fig. 28). This allows a study not only of the intensity distribution, but also of the phase distribution. From the width of this distribution, an independent measure of the diffusion coefficient can be found, which Vellekoop, Lodahl, and Lagendijk [2005] find in good agreement with several other ways of determining D.

When photons are localized within a sample, the phase delay distribution changes accordingly. Due to the presence of closed loops, there will be an increase in constructive interferences of the different paths. In turn

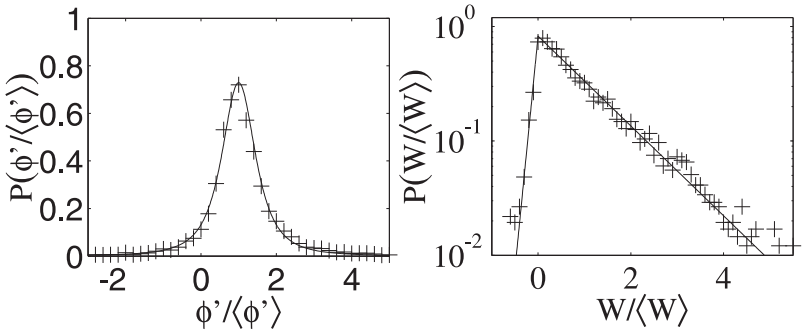

Figure 28: Distribution of the phase delay in a random sample. Left the delay time, right the delay time weighted by the intensity. For classical samples, the width of these distributions yields a measure of the diffusion coefficient of light. In Vellekoop, Lodahl, and Lagendijk [2005], this was done for TiO_2 particles of several sizes and a typical result is shown here. The determiation of the diffusion coefficient in this way agrees very well with that from time-of-flight measurements. Reprinted figure with permission from Vellekoop, Lodahl, and Lagendijk [2005]. Copyright 2005 by the American Physical Society.

this leads to an intensity distribution with a non-exponential tail at high intensities (as well as a suppression at small intensities due to conservation of energy). This has been calculated in one dimensional and quasi-one dimensional systems (Nieuwenhuizen and van Rossum [1995], Sebbah, Hu, Klosner, and Genack [2006]) These calculations are in agreement with the results obtained from microwaves discussed above (Garcia and Genack [1989]), however, the situation in three dimensional systems is less clear. There have as of yet been no experimental findings of a changed phase statistics close to Anderson localization. In addition, there are no explicit calculations for the phase distribution in a three dimensional localizing sample.

3.3. TIME-RESOLVED MEASUREMENTS

As we have seen above, static measurements of transmission or reflections are not readily suited to observe effects of strong localization. This is due to the fact that a simple loss of number of photons in transmission in thick samples cannot distinguish localization from absorption. Therefore, one has be able to determine the phase of the photons as well. This can either be done via a quantification of the fluctuations as discussed above or via time resolved measurements as we will discuss below. Since localization acts differently on photons which have spent a different amount of time inside the sample, localization and absorption can in this case be separated. This can be seen by the different functional dependencies implied by the effects. Absorption invariably leads to an exponential decrease also of the time resolved intensity, while localization and its corresponding renormalization of the diffusion coefficient lead to a decay slower than exponential.

3.3.1. The diffusion coefficient

In a typical time-resolved measurement, the path length distribution of photons inside a sample of finite thickness is obtained. This can be done either in transmission or in reflection. Due to the fact that the time-scale of the signal is much faster in reflection (most of the intensity is only delayed a time l^*/v), an experiment in transmission is much mor feasible. There have however also been experiments in reflection (Johnson, Imhof, Bret, Rivas, and Lagendijk [2003]). In the diffusion approximation, the path length distributions can be calculated analytically. For a derivation see for

instance Lenke and Maret [2000]. In transmission, one obtains:

$$T(t) \propto \sum_n (-1)^{n+1} \exp\left[-\left(\frac{n^2\pi^2 D}{L^2} + \frac{1}{\tau_{abs}}\right) t\right], \tag{3.1}$$

where τ_{abs} is the absorption length. Thus for a sample of given length, the time resolved intensity is solely determined by D and τ_{abs}. These two parameters have very little covariance, as the time delay until sizeable transmission through the sample is achieved is solely determined by D, while the long time behaviour is given by an exponential decay with a slope of $\pi^2 D/L^2 + 1/\tau_{abs}$.

In order to measure the time resolved transmission, several types of setups have been used. Usually, a pulsed laser-system capable of producing ps-pulses shines light on the sample. Behind the sample, a photodetector starts a clock, which is subsequently stopped by a delayed reference pulse. For a more detailed description of such setups see e.g. Watson, Fleury, and McCall [1987], Störzer, Gross, Aegerter, and Maret [2006]. For very thin samples, pulses on the scale of a few fs are needed, such that the detection needs to be done using interferometric methods. This was done by Johnson, Imhof, Bret, Rivas, and Lagendijk [2003] using samples of etched GaP. This will be discussed in more detail below in the context of time resolved reflection measurements. Fig. 29, shows the result of a measurement using a ps system (Störzer, Gross, Aegerter, and Maret [2006]), in the case of a sample of TiO_2 particles of an average diameter of 540 nm at a wavelength of 590 nm. This sample has a value of $kl^* = 6.3(3)$ and thus shows purely diffusive behaviour as can be seen from the red line, which shows a fit to Eq. 3.1, which perfectly describes the data.

Due to the fact that time resolved transmission thus allows a direct determination of the diffusion coefficient, many early experiments have looked for anomalously low values of D, or a thickness dependence of D (see e.g. Watson, Fleury, and McCall [1987], Drake and Genack [1989]). In these experiments, Drake and Genack [1989] have found very low values of D and interpreted them as an indication of the onset of localization (see Fig. 30). However, due to resonance scattering as discussed above, and pointed out by van Albada, van Tiggelen, Lagendijk, and Tip [1991] a low value of D does not necessarily imply a low value of l^* nor the onset of localization. This is because the reduction in transport velocity induced by the increased dwell time in resonance scattering will reduce the value of D obtained from time of flight measurements.

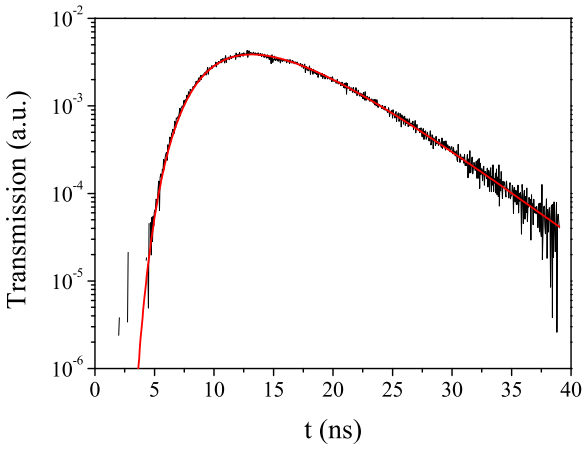

Figure 29: Time-resolved transmission for a classical sample with $kl^* = 6.3$ (data from Störzer, Gross, Aegerter, and Maret [2006]). The full red line is a fit to classical diffusion theory through a slab of length L, which allows a determination of the diffusion coefficient and the absorption length. There is little covariance between the two quantities as D determines the time lag before any photons are transmitted through the sample, while the absorption length only influences the slope of the exponential long-time tail.

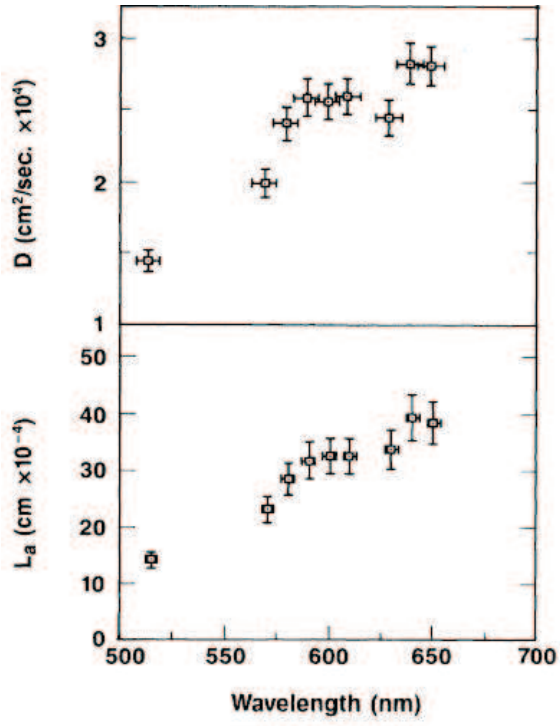

Figure 30: The diffusion coefficient and the absorption length of light trough powders of TiO_2 as determined by time of flight measurements Drake and Genack [1989]. The decrease of the diffusion coefficient with incident wavelength was interpreted as the onset to the localization transition, which predicts a vanishing of the diffusion coefficient at a phase transition with kl^*, i.e. the wavelength. However it has later been shown van Albada, van Tiggelen, Lagendijk, and Tip [1991] that such a decrease is more likely due to an increased dwell time caused by resonant scattering of the particles having roughly the same size as the wavelength of light. Reprinted figure with permission from Drake and Genack [1989]. Copyright 1989 by the American Physical Society.

Similar information can also be gathered from a time-resolved measurement in reflection geometry. In this case, there are additional experimental difficulties due to the much shorter time scales of the reflection signal. In reflection, most photons exit the sample after very few scattering events, therefore the peak in the time-resolved intensity is of the order of l/v, where l is the scattering mean free path. For samples close to the localization transition, i.e. with a mean free path comparable to the wavelength, this time is of the order of a few fs and thus very difficult to measure. After this peak, it can again be calculated in the diffusion approximation (see Johnson, Imhof, Bret, Rivas, and Lagendijk [2003]) that the intensity decreases as:

$$R(t) \propto \sum_n n^2 \exp\left[-\left(\frac{n^2\pi^2 D}{L^2} + \frac{1}{\tau_{abs}}\right)t\right] \tag{3.2}$$

For short times this corresponds to a power-law decay with an exponent of 3/2, whereas at long times (the time scale of transmission) there is an exponential decay on the same time-scale as in transmission measurements. Due to the time-scale of the resulting intensity, measurements of time-resolved reflection need to be done with a fs-pulsed laser and the signal needs to be recorded interferometrically. In addition, the fact that most signal will be from photons which only have gone through a few scattering events, the signal to noise will limit the time resolution to which reflection measurements can be performed. In spite of these differences, Johnson, Imhof, Bret, Rivas, and Lagendijk [2003] have carried out measurements of time-resolved reflection on porous GaP samples with very small values of kl^*. The result is shown in Fig. 31, where one can clearly see the initial power-law decay and the subsequent exponential decrease due to the finite sample and a possible absorption.

Measurements of the diffusion coefficient from such time-resolved measurements, both in transmission and reflection do show good agreement with determinations from the phase fluctuations as found by Vellekoop, Lodahl, and Lagendijk [2005].

3.3.2. Spatially dependent diffusion coefficient

Since time-resolved measurements of transmission or reflection are capable of determining the diffusion coefficient very accurately, it is also possible to employ such measurements in the search for a scale dependence of the diffusion coefficient. One of the hallmarks of localization, as discussed above,

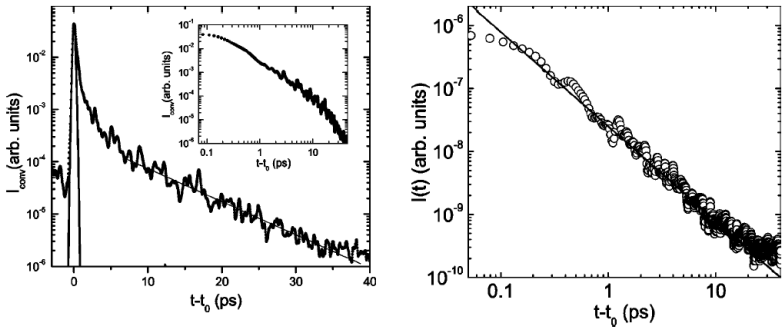

Figure 31: Time resolved measurements of reflection (data from Johnson, Imhof, Bret, Rivas, and Lagendijk [2003]). The left panel shows the data on a logarithmic scale showing the exponantial decrease at long times due to finite thickness and absorption. On the right the same data are shown on a double-logarithmic scale after deconvolution with the pulse shape. This demonstrates that at shorter times, the data can be described by a power-law decay with an exponent of 3/2 (straight line) in agreement with diffusion theory. Reprinted figure with permission from Johnson, Imhof, Bret, Rivas, and Lagendijk [2003]. Copyright 2003 by the American Physical Society.

is that the diffusion coefficient becomes renormalized (Abrahams, Anderson, Licciardello, and Ramakrishnan [1979]). This renormalization with the scale of the sample can be translated into a path length dependence of the diffusion coefficient, as was first calculated by Berkovits and Kaveh [1987] at the critical point. Subsequently, they inserted this path-length dependence into the diffusion theory of time-resolved transmission (Berkovits and Kaveh [1990]). This changes the classical expectation (Eq. 3.1) to

$$T(t) \propto \sum_n (-1)^{n+1} \left(\frac{D(t)}{D_0} \right)^2 \exp \left[- \left(\frac{n^2 \pi^2 D(t)}{L^2} + \frac{1}{\tau_{abs}} \right) t \right], \qquad (3.3)$$

Similarly, a path-length dependence of the diffusion coefficient was used to calculate the influence of localization on the cone shape discussed above (van Tiggelen, Lagendijk, and Wiersma [2000]). Later investigations by some of these authors (Skipetrov and van Tiggelen [2004], Skipetrov and van Tiggelen [2006]) on self-consistent theory in open systems have explicitly calculated the effect of localization on time-resolved measurements. In reflection geometry, they find a change of the exponent of the power-law decay from 3/2 to 2 as the localization transition is crossed (Skipetrov and van Tiggelen [2004]). This will however be extremely difficult to observe experimentally. As discussed above, reflection measurements have to be done on short time scales and are limited by signal to noise due to high intensities at very short times. In addition, absorption and a finite sample will also lead to a decrease in intensity from the $t^{-3/2}$ power-law, which will be exceedingly difficult to distinguish from a t^{-2} predicted from localization theory. In transmission, Skipetrov and van Tiggelen [2004] find a similar result to Berkovits and Kaveh [1990] in that the path length dependence of the diffusion coefficient leads to a non-exponential tail in time-resolved transmission with a decreasing slope. In addition to Berkovits and Kaveh [1990], Skipetrov and van Tiggelen [2004] also explicitly study the effect of the dimensionality. Consistent with scaling theory of Abrahams, Anderson, Licciardello, and Ramakrishnan [1979], they find that in quasi-one dimension, effects of localization can already be observed above the transition (Skipetrov and van Tiggelen [2004]). With this it is possible for instance to describe the results on micro-wave transmission (Chabanov, Zhang, and Genack [2003]), discussed above. In three-dimensional systems however, no signs of localization are observed above the transition at all (Skipetrov and van Tiggelen [2006]).

In Fig. 32, we show time-resolved transmission measurements of a TiO_2 sample with a value of $kl^* \simeq 2.5$ (Störzer, Gross, Aegerter, and Maret

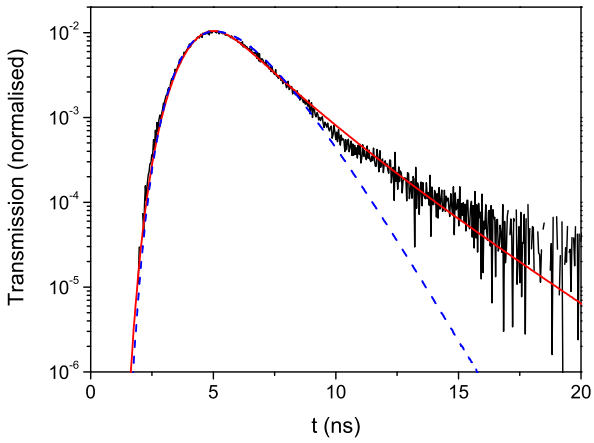

Figure 32: Time-resolved transmission of a localizing sample with $kl^* = 2.5$ (data from Störzer, Gross, Aegerter, and Maret [2006]). As can be seen, the transmitted intensiy at long times shows a non-exponential tail indicative of a renormalized diffusion coefficient (see figure 33). In fact, the full red line is a fit to diffusion theory including a scale dependent diffusion coefficient as done in Aegerter, Störzer, and Maret [2006]. For comparison, a fit to classical diffusion including absorption is shown by the dashed blue line.

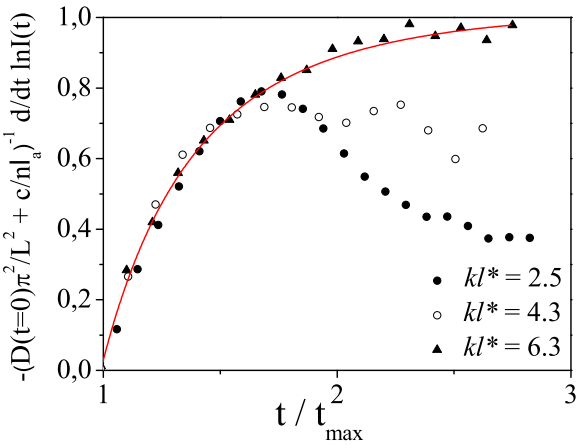

Figure 33: The long time behaviour of time-of-flight measurements allows a direct determination of the spatial dependence of the diffusion coefficient. Taking the negative time-derivative of the logarithm of the transmitted intensity one obtains an effective diffusion coefficient, which at long times should be constant. This is shown here for three different samples, where the sample with $kl^* = 6.3$ agrees perfectly with diffusion theory and a constant diffusion coefficient. The sample with $kl^* = 2.5$ however shows a decrease of the diffusion coefficient at long times.

[2006]), the particles have a diameter of 250 nm. As can be seen, the transmission in this sample cannot be described by classical diffusion (Eq. 3.1, shown by the dashed blue line) alone. There is a non exponential decay with a decreasing slope as predicted by localization theory. This can be quantified in the same way as has been done by Chabanov, Zhang, and Genack [2003] as well as Skipetrov and van Tiggelen [2004], by taking the negative derivative of the log of the transmission data. This is shown in Fig. 33 for several samples with varying values of kl^*. As can be seen there, with decreasing kl^*, there are increasing deviations from classical diffusion theory (solid red line). This is however only a qualitative measure of possible signs of localization and a more quantitative description is still needed. Unfortunately, the predictions of Skipetrov and van Tiggelen [2006] cannot

be directly compared to the data, as the samples are much thicker than can be described theoretically. However, using the analytic description of Berkovits and Kaveh [1990] (Eq. 3.3) it is possible to obtain a path-length dependence of the diffusion coefficient from the data by way of a fit with $D(t)$. This is shown by the solid red line in Fig. 32, which describes the data reasonably well. The time dependence of $D(t)$ obtained from this fit, is consistent with earlier simulation results by Lenke, Tweer, and Maret [2002], where a self-attracting random walk was simulated and effective diffusion coefficients were determined. The result of these simulations in three dimensions shows that the diffusion coefficient is constant for some time after which it decreases as $1/t$. This is the same behaviour which was used to obtain the fit in Fig. 32. Such a behaviour can be physically explained from the fact that up to the localization length, roughly given by the size of closed loops, the diffusion must be classical, as interference effects only appear after a closed loop has been traversed. At later times, the photons are localized to a specific region in space, such that $\langle r^2 \rangle$ tends towards a constant. Describing this behaviour with an effective $D(t)$ immediately leads to a dependence of $D(t) \propto 1/t$. This allows a quantitative discussion not only of the time-resolved transmission experiments and a determination of the localization length discussed below, but also the static transmission measurements discussed above.

The fact that Johnson, Imhof, Bret, Rivas, and Lagendijk [2003] have not found a non-exponential decay in their time-resolved measurements while their samples had similar values of kl^* is probably due to the small thicknesses used in that study. As can be seen from Fig. 32, in the TiO_2 samples, localization effects only start to appear after a few ns. This corresponds to roughly a million scattering events. Comparing this to the transmission data of Johnson, Imhof, Bret, Rivas, and Lagendijk [2003], this is almost an order of magnitude bigger than their maximum time of flight (their maximum sample thickness is 20μm). More quantitatively, this is connected to the size of the localization length discussed below.

3.3.3. The localization length

Given the phenomenological description of the diffusion coefficient based on the simulations of the self-attracting random walk discussed above (Lenke, Tweer, and Maret [2002]), the deviations from the diffusion picture in time resolved measurements can be quantified. In the localized state, the effective diffusion coefficient will decrease $\propto 1/t$, which corresponds to a limited

extent of the photon cloud. On the other hand, above the transition, the diffusion coefficient should be constant. This implies that a systematic study of the deviations from classical diffusion with decreasing kl^* should show a transition between these two asymptotic behaviours. In this case, the localization length would simply be given by $\sqrt{D_0\tau_{loc}}$, which however can only be determined as long as this length scale is smaller than the sample thickness.

Considering the predictions of one-parameter scaling theory however, the situation is somewhat more complicated. The fact that D is renormalized to be dependent on the sample thickness as $1/L$ has been translated to a path length dependence by Berkovits and Kaveh [1990] to imply a path length dependence as $D(t) \propto t^{-1/3}$. To take this into account, the time of flight measurements have been fitted with a power-law dependence of $D(t) \propto t^{-a}$ at long times (Aegerter, Störzer, and Maret [2006]). In the approach to localization, this exponent increases from its classical value of zero to its localized value of one. At the transition, even the exponent of $1/3$ can be observed, showing the critical point renormalization of the diffusion coefficient, see Fig. 34. This plot also shows that indeed the exponent is given by one at low values of kl^*, corresponding to a localized state, while it is zero above the transition. This transition can be determined from the dependence of the localization exponent in the figure to be $kl_c^* \simeq 4$.

The algebraic decay of the diffusion coefficient in the critical regime does complicate the determination of the localization length somewhat. Due to the fact that a classical behaviour can be obtained also from a change in the exponent, the localization length now has to be determined via $L^{1-a}\sqrt{D_0\tau_{loc}}^a$. In the limiting cases of a = 1,0 this gives the same values as above, while giving an interpolation in the critical regime. The inverse of the localization length is the order parameter in the transition to localization. Therefore a systematic study of the localization length as a function of kl^* gives a description of the transition including the critical point and the critical exponent.

In Fig. 35, this dependence is plotted with the localization length normalized to the sample thickness. For a finite sample, localization can only be observed if the localization length is smaller than the sample thickness. Therefore, very thin samples having values of kl^* below the transition will not show effects of localization and only very thick samples (with L far exceeding 100 l^*) can show the underlying transition. This is probably why the time of flight measurements of Johnson, Imhof, Bret, Rivas, and Lagendijk [2003] are well described by classical diffusion in spite of the fact

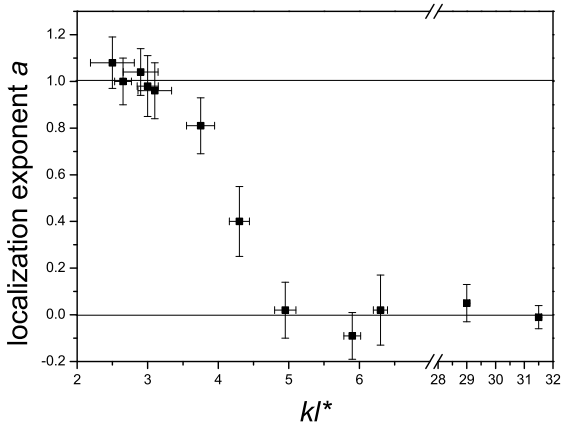

Figure 34: The scale dependence of the diffusion coefficient can be quantified by the exponent, a, with which D decreases as a function of time. Its value is plotted here as a function of kl^* (data from Aegerter, Störzer, and Maret [2006]). As can be seen, above the transition to localization, the diffusion coefficient is constant as indicated by an exponent of $a = 0$, whereas below $kl^* \simeq 4$ it increases to $a = 1$, which corresponds to a localized state.

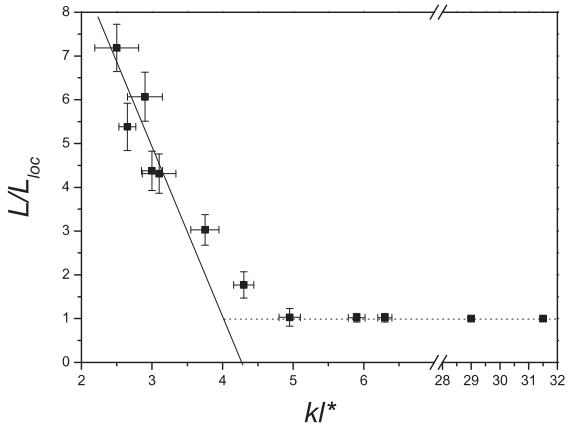

Figure 35: The dependence of the inverse localization length on the critical parameter kl^* (adapted from Aegerter, Störzer, and Maret [2006]). Below a critical value of $kl_c^* \simeq 4$, the localization length as given by $\sqrt{D_0\tau_l}$ becomes smaller than the sample thickness indicating the transition to a macroscopic population of localized states.

that their values of kl^* are close to or beyond the transition. Their samples, which consist of photoanodically etched GaP already discussed above in the context of cone-tip measurements are rather thin ($L \simeq 40l^*$). This implies that the paths of the light traversed inside the sample are not long enough to form enough closed loops and thus show localization.

3.3.4. Determination of the critical exponent

The systematic determination of the localization length for different samples around the localization transition also allows an experimental investigation of the critical exponent (Aegerter, Störzer, and Maret [2006]). In this context, scaling theory (Abrahams, Anderson, Licciardello, and Ramakrishnan [1979]) predicts a critical exponent $\nu < 1$, without specifying a precise value. As discussed above, an epsilon expansion in the dimension starting from the lower critical dimension ($d_l = 2$) yields a value of 1/2 for the critical exponent (John [1984]), however due to the fact that the system considered here is fully three dimensional, such a comparison cannot be considered precise. However, the fact that above the upper crit-

ical dimension ($d_u = 4$) the mean-field value $\nu = 1/2$ is always obtained for the exponent of the order parameter in a second order phase transition (Schuster [1978]) would indicate that the value for a three dimensional system should not be too far from these two limiting cases. In contrast, numerical evaluations of the Green-Kubo formalism consistently obtain a value of $\nu = 1.5$ (MacKinnon and Kramer [1981], Lambrianides and Shore [1994], Rieth and Schreiber [1997]), which is not only inconsistent with the experimental data shown below, but also with one-parameter scaling theory (Abrahams, Anderson, Licciardello, and Ramakrishnan [1979]). It should be noted however that these numerical investigations are carried out on quasi-periodic lattices. As such they thus do not necessarily conform to the nature of Anderson localization, which is fundamentally based on a completely disordered structure. This may explain the discrepancy with the analytic as well as the experimental results.

When plotting the inverse localization length against the critical parameter $|kl^* - kl_c^*|/kl^*$, Aegerter, Störzer, and Maret [2006] obtain a divergence as shown in Figure 36, with a critical exponent of $\nu = 0.45(10)$. This uses a critical parameter as defined by Berkovits and Kaveh [1990], while John [1984] and others have used a different critical exponent, namely $|kl^* - kl_c^*|$. Using this critical parameter, the data yield a different exponent, namely $\nu = 0.65(15)$. The critical value of kl^* is unaffected by the choice of critical parameter. Such an experimental determination can be used to test the different kinds of theoretical predictions discussed above. One notes that the result is consistent with the rather unspecific prediction of one-parameter scaling theory. Furthermore, it is in striking agreement with the result of the ϵ expansion, as well as the mean field prediction. This is somewhat surprising given that the experiments are carried out in a system of intermediate dimensionality, where both the ϵ expansion and the mean-field result should not explicitly hold. The numerical results finally are strongly inconsistent with the data, which might be due to the fact that the numerical results are obtained from quasi-periodic systems.

§ 4. Conclusions and outlook

Watching the light scattered back from an object can not only give a wealth of information on the scattering object, but also on some properties of light itself. As long as the scatterers are sufficiently random and the samples thus opaque, the photonic analogue of the metal-insulator transition can be observed. Due to the fact that in this case, there is no interaction between

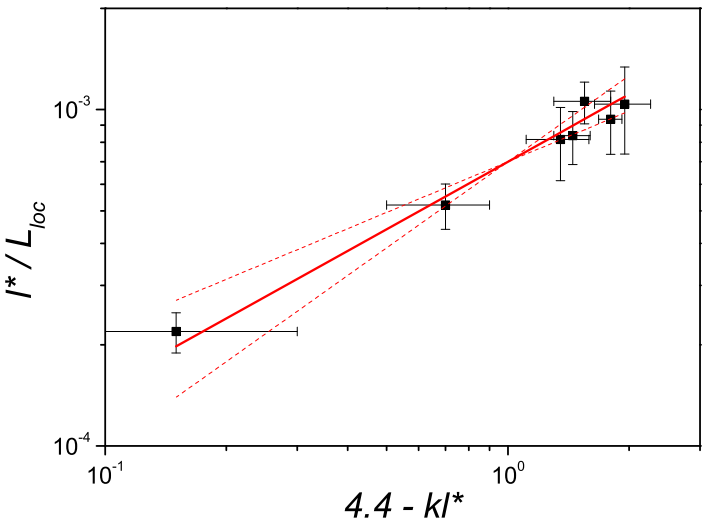

Figure 36: The inverse localization length as a function of the critical parameter $|kl^* - kl_c^*|$. As can be seen, the localization length diverges in the approach to a citical point at $kl_c^* = 4.4(2)$ with an exponent ν consistent with a value of 0.65(15) (full line in the figure). This is in accord with a mean-field argument for the value of the ctitical exponent but in contradiction with numerical simulations (MacKinnon and Kramer [1981]).

the diffusing particles, i.e. the photons in contrast to the electrons in a metal, a theoretic treatment of photon localization is closer than that of electrons.

As we have seen however, great care has to be taken in the experimental investigation of photon localization. Absorption, resonant scattering or other external effects may well pose as localization in that they also produce an exponential decrease in transmission or a slowing down of transport respectively. Therefore, investigations of localization have to concentrate on measures that are unaffected by absorption or transport speed, such as the speckle intensity distribution or time resolved measurements. On the other hand, static measures are still useful, however in that case one needs an independent quantification of the absorption and the transport speed.

Using time-resolved measurements, Störzer, Gross, Aegerter, and Maret [2006] have found clear indications of non-classical diffusion, which show all the hallmarks of localization and cannot be explained by the above artefacts. In fact a quantitative description of these data by Aegerter, Störzer, and Maret [2006] with qualitative localization theory not only finds localized states as given by a constant $\langle r^2 \rangle$, but can also describe the thickness dependence of the static transmission over twelve orders of magnitude without a single adjustable parameter. However, these measurements cannot give evidence to the interference nature of the effect. For this purpose, measurements affecting the phase of the propagating photons would be necessary. In this context, it is useful to remember the work of Erbacher, Lenke, and Maret [1993] and Golubentsev [1984], showing that weak localization can be destroyed by the application of a strong magnetic field to a Faraday-active multiple scattering medium. Using the same approach, it might be possible to add a Faraday active material to a sample showing localization and apply a strong magnetic field. A destruction of the non-exponential tail in this case would clearly show the interference nature of the effect and thus Anderson localization. Work to this effect is under way.

§ 5. Acknowledgements

We would like to thank all the current and previous members of the localization team in Konstanz/Strasbourg/Grenoble for their efforts over the years in studying multiple scattering. Without their work many results presented here would not have been possible. In particular, we thank M. Störzer, S. Fiebig, W. Bührer, P. Gross, R. Tweer, R. Lenke, R. Lehner, C. Eisenmann, D. Reinke, U. Mack, F. Scheffold, F. Erbacher, and P.E. Wolf.

In addition we would like to thank many colleagues for valuable discussions on pertinent questions as well as for making available some of their data to be presented here. These are E. Akkermans, N. Borisov, M. Fuchs, A.Z. Genack, M.D. Havey, R. Kaiser, A. Lagendijk, R. Maynard, G. Montambaux, M. Noginov, J. Pendry, P. Sebbah, P. Sheng, S.E. Skipetrov, H. Stark, B. van Tiggelen, D.S. Wiersma.

Finally, this work is currently funded by the International Research Training Group "Soft Condensed Matter Physics of Model Systems" by the DFG and the Centre of Applied Photonics jointly financed by Ministry of Science, Research and Arts of Baden-Württemberg as well as the University of Konstanz. We are very grateful for their contributions.

§ References

Abrahams, Anderson, Licciardello, and Ramakrishnan [1979]
E. Abrahams, P.W. Anderson, D. Licciardello, T.V. Ramakrishnan, 1979, Scaling theory of localization: absence of quantum diffusion in two dimensions, Phys. Rev. Lett. **42**, 673–676.

Aegerter, Störzer, and Maret [2006]
C.M. Aegerter, M. Störzer, and G. Maret, 2006, Experimental determination of critical exponents in Anderson localization of light, Europhys. Lett. **75**, 562–568.

Aegerter, Störzer, Fiebig, Bührer, and Maret [2007]
C.M. Aegerter, M. Störzer, and G. Maret, 2007, Observation of Anderson localization of light in bulk 3D systems, J. Opt. Soc. Am. to be published.

Akkermans, Wolf, and Maynard [1986]
E. Akkermans, P.E. Wolf, and R. Maynard, 1986, Coherent Backscattering of Light by Disordered Media: Analysis of the Peak Line Shape, Phys. Rev. Lett. **56**, 1471–1474.

Akkermans, Wolf, Maynard and Maret [1988]
E. Akkermans, P.E. Wolf, R. Maynard and G. Maret, 1988, Theoretical study of the coherent backscattering of light by disordered media, J. de Physique (France), **49**, 77–98.

Akkermans and Montambaux [2006]
E. Akkermans and G. Montambaux, 2006, Mesoscopic Physics of electrons and photons, Cambridge University Press.

Altshuler and Lee [1988]
B.L. Altshuler and P.A. Lee, 1988, Disordered electronic systems, Physics Today, p. 36, december.

Anderson [1958]
P.W. Anderson, 1958, Absence of diffusion in certain random lattices, Phys. Rev. **109**, 1492–1505.
Anderson [1985]
P.W. Anderson, 1985, The question of classical localization: a theory of white paint?, Phil. Mag. B **52**, 505–509.
Bayer and Niederdränk [1993]
G. Bayer and T. Niederdränk, 1993, Weak localization of acoustic waves in strongly scattering media, Phys. Rev. Lett. **70**, 3884–3887.
G. Bergmann [1984]
G. Bergmann, 1984, Weak-localisation in thin films, Phys. Rep. **107**, 1–58.
Berkovits and Kaveh [1987]
R. Berkovits and M. Kaveh, 1987, Backscattering of light near the optical Anderson transition, Phys. Rev. B **36**, 9322–9325.
Berkovits and Kaveh [1990]
R. Berkovits and M. Kaveh, 1990, Propagation of waves through a slab near the Anderson transition: a local scaling approach, J. Phys.:Cond Mat. **2**, 307–321.
Bidel, Klappauf, Bernard, Delande, Labeyrie, Miniatura, Wilkowski, and Kaiser [2002]
Y. Bidel, B. Klappauf, J.C. Bernard, D. Delande, G. Labeyrie, C. Miniatura, D. Wilkowski, and R. Kaiser, 2002, Coherent Light Transport in a Cold Strontium Cloud, Phys. Rev. Lett. **88**, 203902 (1–4).
Bryant and Jarmie [1974]
H.C. Bryant and N. Jarmie, 1974, The glory, Sci. Am. **231(1)**, 60-71.
Busch and Soukoulis [1996]
K. Busch and C.M. Soukoulis, 1996, Transport properties of random media: An energy-density CPA approach, Phys. Rev. B **54**, 893–899.
Campillo and Paul [2003]
M. Campillo and A. Paul, 2003, Long-Range Correlations in the Diffuse Seismic Coda, Science **299**, 547–549.
Chabanov, Stoytchev, and Genack [2000]
A.A. Chabanov, M. Stoytchev, and A.Z. Genack, 2000, Statistical signatures of photon localization, Nature (London) **404**, 850–853.
Chabanov and Genack [2001]
A.A. Chabanov and A.Z. Genack, 2001, Statistics of Dynamics of Localized Waves, Phys. Rev. Lett. **87**, 153901 (1–4).
Chabanov, Zhang, and Genack [2003]
A.A. Chabanov, Z.Q. Zhang, and A.Z. Genack, 2003, Breakdown of Diffusion in Dynamics of Extended Waves in Mesoscopic Media, Phys. Rev. Lett. **90**, 203903 (1–4).
Cheung, Zhang, Zhang, Chabanov, and Genack [2004]
S.K. Cheung, X. Zhang, Z.Q. Zhang, A.A. Chabanov, and A.Z. Genack, 2004,

Impact of Weak Localization in the Time Domain, Phys. Rev. Lett. **92**, 173902 (1–4).

Clément, Varón, Hugbart, Retter, Bouyer, Sanchez-Palencia, Gangardt, Shlyapnikov, and Aspect [2005]

D. Clement, A.F. Varon, M. Hugbart, J.A. Retter, P. Bouyer, L. Sanchez-Palencia, D.M. Gangardt, G.V. Shlyapnikov, and A. Aspect, 2005, Phys. Rev. Lett. **95**, 170409 (1–4).

Descartes [1637]

R. Descartes, 1637, Discours de la Méthode Pour Bien Conduire Sa Raison et Chercher la Vérité dans les Sciences (second appendix) La Dioptrique.

Drake and Genack [1989]

J.M. Drake and A.Z. Genack, 1989, Observation of nonclassical optical diffusion, Phys. Rev. Lett. **63**, 259–262.

Erbacher, Lenke, and Maret [1993]

F.A. Erbacher, R. Lenke, G. Maret, 1993, Multiple light scattering in magneto-optically active media, Europhys. Lett. **21**, 551–557.

Faraday [1846]

M. Faraday, 1846, On the Magnetization of Light and the Illumination of Magnetic Lines of Force, Phil. Trans. Roy. Soc. **136**, 1–20.

Fiebig, Aegerter, Bührer, Störzer, Montambaux, Akkermans and Maret [2007]

S. Fiebig, C.M. Aegerter, W. Bührer, M. Störzer, G. Montambaux, E. Akkermans and G. Maret, 2007, Conservation of energy in coherent backscattering of light, to be published.

Fraden and Maret [1990]

S. Fraden, and G. Maret, 1990, Multiple light scattering from concentrated, interacting suspensions, Phys. Rev. Lett. **65**, 512–515.

Fraser [1994]

A.B. Fraser, 1994, The sylvanshine: retroreflection from dew-covered trees, Appl. Opt. **33** 4539-4547.

Garcia and Genack [1989]

N. Garcia and A.Z. Genack, 1989, Crossover to strong intensity correlation for microwave radiation in random media, Phys. Rev. Lett. **63**, 1678–1981.

Garnett [1904]

J.C.M. Garnett, 1904, Colours in metal glasses and in metallic films, Phil. Trans. R. Soc. A **203**, 385–420.

Gehrels [1956]

T. Gehrels, 1956, Photometric studies of asteroids; V. The lightcurve and phase function of 20 Massalia, Astrophysical Journal **123**, 331–338.

Genack [1987]

A.Z. Genack, 1987, Optical transmission in disordered media, Phys. Rev. Lett. **58**, 2043–2046.

Genack and Garcia [1991]
A.Z. Genack and N. Garcia, 1991, Observation of photon localization in a three-dimensional disordered system, Phys. Rev. Lett. **66**, 2064–2067.

Golubentsev [1984]
A.A. Golubentsev, 1984, Suppression of interference effects in multiple scattering of light, Sov. Phys. JETP **59**, 26–32.

Gross [2005]
P. Gross, 2005, Coherent backscattering close to the transition to strong localization of light, Diploma Thesis, Univ. of Konstanz.

Gross, Störzer, Fiebig, Clausen, Maret, and Aegerter [2007]
P. Gross, M. Störzer, S. Fiebig, M. Clausen, G. Maret, and C.M. Aegerter, 2007, A precise method to determine the angular distribution of backscattered light to high angles, Rev. Sci. Instr. **78**, 033105.

Hapke, Nelson and Smythe [1993]
B.W. Hapke, R.M. Nelson and W.D. Smythe, 1993, The opposition effect of the Moon : the contribution of coherent backscattering, Science **260**, 509–511.

Hikami [1981]
S. Hikami, 1981, Anderson localization in a nonlinear-σ-model representation, Phys. Rev. B **24**, 2671–2679.

Igarashi [1987]
J-I. Igarashi, 1987, Coherent backscattering of neutrons, Phys. Rev. B **35**, 8894–8897.

Ioffe and Regel [1960]
A.F. Ioffe and A.R. Regel, 1960, Non-crystalline, amorphous and liquid electronic semiconductors, Progress in Semiconductors **4**, 237–291.

Ishimaru and Tsang [1988]
A. Ishimaru and L. Tsang, 1988, Backscattering enhancement of random discrete scatterers of moderate sizes, J. Opt. Soc. Am. A, **5(2)**, 228–236.

John [1984]
S. John, 1984, Electromagnetic Absorption in a Disordered Medium near a Photon Mobility Edge, Phys. Rev. Lett. **53**, 2169–2172.

John [1985]
S. John, 1985, Localization and absorption of waves in a weakly dissipative disordered medium, Phys. Rev. B **31**, 304–309.

John [1987]
S. John, 1987, Strong Localization of Photons in Certain Disordered Dielectric Superlattices, Phys. Rev. Lett. **58**, 2486–2489.

Johnson, Imhof, Bret, Rivas, and Lagendijk [2003]
P.M. Johnson, A. Imhof, B.P.J. Bret, J.G. Rivas, and A. Lagendijk, 2003, Time resolved pulse propagation in a strongly scattering material, Phys. Rev. E **68**, 016604 (1–9).

Jonckheere, Mller, Kaiser, Miniatura, and Delande [2000]
T. Jonckheere, C.A. Mller, R. Kaiser, C. Miniatura, and D. Delande, 2000, Multiple Scattering of Light by Atoms in the Weak Localization Regime, Phys. Rev. Lett. **85**, 4269–4272.

Kirkpatrick [1985]
T.R. Kirkpatrick, 1985, Localization of acoustic waves, Phys. Rev. B **31**, 5746–5755.

Klitzing, Dorda, and Pepper [1980]
K. v. Klitzing, G. Dorda, and M. Pepper, 1980, New method for high-accuracy determination of the fine-structure constant based on quantized Hall resistance, Phys. Rev. Lett. **45**, 494–497.

Kogan, Kaveh, Baumgartner, and Berkovits [1993]
E. Kogan, M. Kaveh, R. Baumgartner, and R. Berkovits, 1993, Statistics of waves propagating in a random medium Phys. Rev. B **48**, 9404–9407.

Kogan and Kaveh [1995]
E. Kogan and M. Kaveh, 1995, Random-matrix theory approach to the intensity distributions of waves propagating in a random medium, Phys. Rev. B **52**, R3813–R3815.

Kuga and Ishimaru [1984]
Y. Kuga and A. Ishimaru, 1984, Retroreflectance from a dense distribution of spherical particles, J. Opt. Soc. Am. A, **1(8)**, 831–835.

Kuhn, Miniatura, Delande, Sigwarth, and Müller [2005]
R.C. Kuhn, C. Miniatura, D. Delande, O. Sigwarth, and C.A. Müller, 2005, Localization of Matter Waves in Two-Dimensional Disordered Optical Potentials, Phys. Rev. Lett. **95**, 250403 (1–4).

Kupriyanov, Sokolov, Kulatunga, Sukenik, and Havey [2003]
D.V. Kupriyanov, I.M. Sokolov, P. Kulatunga, C.I. Sukenik, and M.D. Havey, 2003, Coherent backscattering of light in atomic systems: Application to weak localization in an ensemble of cold alkali-metal atoms, Phys. Rev. A **67**, 013804 (1–13).

Labeyrie, de Tomasi, Bernard, Müller, Miniatura and Kaiser [1999]
G. Labeyrie, F. de Tomasi, J.-C. Bernard, C.A. Müller, Ch. Miniatura and R. Kaiser, 1999, Coherent backscattering of light by cold atoms, Phys. Rev. Lett. **83**, 5266–5269.

Labeyrie, Delande, Müller, Miniatura and Kaiser [2003]
G. Labeyrie, D. Delande, C.A. Müller, C. Miniatura and R. Kaiser, 2003, Coherent backscattering of light by cold atoms : Theory meets experiment, Europhys. Lett., **61**, 327–333.

Labeyrie, Vaujour, Müller, Delande, Miniatura, Wilkowski and Kaiser [2003]
G. Labeyrie, E. Vaujour, C.A. Müller, D. Delande, C. Miniatura, D. Wilkowski and R. Kaiser, 2003, Slow Diffusion of Light in a Cold Atomic Cloud, Phys. Rev. Lett., **91**, 223904 (1–4).

Lagendijk, Vreeker, and de Vries[1989]
A. Lagendijk, R. Vreeker, and P. de Vries, 1989, Influence of internal reflection on diffusive transport in strongly scattering media, Phys. Lett. A **136**, 81–88.

Lambrianides and Shore [1994]
P. Lambrianides and H.B. Shore, 1994, Numerical-scaling experiments in Anderson localization, Phys. Rev. B **50** 7268–7271.

Larose, Margerin, van Tiggelen, and Campillo [2004]
E. Larose, L. Margerin, B.A. van Tiggelen, and M. Campillo, 2004, Weak Localization of Seismic Waves, Phys. Rev. Lett. **93**, 048501 (1–4).

Laughlin [1983]
R. B. Laughlin, 1983, Anomalous quantum Hall effect: An incompressible quantum fluid with fractionally charged excitations, Phys. Rev. Lett. **50**, 1395–1398.

Lee and Ramakrishnan [1985]
P.A. Lee and T.V. Ramakrishnan, 1985, Disordered electronic systems, Rev. Mod. Phys. **57**, 287–337.

Lenke and Maret [2000]
R. Lenke and G. Maret, 2000, Magnetic Field Effects on Coherent Backscattering of Light, Europ. Phys. J. B. **17**, 171–185.

Lenke, Lehner and Maret [2000]
R. Lenke, R. Lehner, and G. Maret, 2000, Magnetic-field effects on coherent backscattering of light in case of Mie spheres Europhys. Lett. **52**, 620–626.

Lenke and Maret [2000]
R. Lenke and G. Maret, 2000, Multiple Scattering of Light: Coherent Backscattering and Transmission in *Scattering in Polymeric and Colloidal Systems*, Brown, W., Mortensen, K., Eds. (Gordon and Breach Scientific, New York), chap 1.

Lenke, Mack, and Maret [2002]
R. Lenke, U. Mack, and G. Maret, 2002, Comparison between "The Glory" and Coherent Backscattering of Light in turbid Media, J. Opt. A: Pure Appl. Opt. **4**, 309–314.

Lenke, Eisenmann, Reinke, and Maret [2002]
R. Lenke, C. Eisenmann, D. Reinke, and G. Maret, 2002, Measurement of the magneto-optical correlation length in turbid media, Phys. Rev. E **66**, 056610 (1–4).

Lenke, Tweer, and Maret [2002]
R. Lenke, R. Tweer, and G. Maret, 2002, Coherent Backscattering and Localization in a Self-attracting Random Walk Model, Eur. Phys. J. B **26**, 235–240.

Lye, Fallani, Modugno, Wiersma, Fort, and Inguscio [2005]
J. E. Lye, L. Fallani, M. Modugno, D.S. Wiersma, C. Fort, and M. Inguscio, 2005, Bose-Einstein Condensate in a Random Potential, Phys. Rev. Lett. **95**, 070401 (1–4).

Maret and Wolf [1987]

G. Maret and P.E. Wolf, 1987, Multiple light scattering from disordered media. The effect of brownian motion of scatterers, Z. Phys. **65**, 409–413.

MacKinnon and Kramer [1981]

A. MacKinnon and B. Kramer, 1981, One-parameter scaling of localization length and conductance in disordered systems, Phys. Rev. Lett. **47**, 1546–1549.

MacKintosh and John [1988]

F.C. MacKintosh and S. John, 1988, Coherent backscattering of light in the presence of time-reversal-noninvariant and parity-nonconserving media, Phys. Rev. B **37**, 1884–1897.

Mie [1908]

G. Mie, 1908, Beiträge zur Optik Trüber Medien, speziell kolloidaler Metallösungen, Ann. Phys. **25**, 377–445.

Müller, Jonckheere, Miniatura, and Delande [2001]

C.A. Müller, T. Jonckheere, C. Miniatura, D. Delande, 2001, Weak localization of light by cold atoms : the impact of quantum internal structure, Phys. Rev. A **64**, 053804.

Nieuwenhuizen and van Rossum [1995]

Th.M. Nieuwenhuizen and M.C.W. van Rossum, 1995, Intensity Distributions of Waves Transmitted through a Multiple Scattering Medium, Phys. Rev. Lett. **74**, 2674 – 2677.

Oetking [1966]

P. Oetking, 1966, Photometric studies of diffusely reflecting surfaces with application to the brightness of the moon, J. Geophys. Res., **71(10)**, 2505–2513.

Page [2007]

J.H. Page, 2007, private communication.

Pine, Weitz, Chaikin, and Herbolzheimer [1988]

D.J. Pine, D.A. Weitz, P.M. Chaikin, and E. Herbolzheimer, 1998, Diffusing wave spectroscopy, Phys. Rev. Lett. **60**, 1134–1137.

Rieth and Schreiber [1997]

T. Rieth and M. Schreiber, 1997, The Anderson transition in three-dimensional quasiperiodic lattices: finite-size scaling and critical exponent, Z. Phys. B **104**, 99-102.

Rikken and van Tiggelen [1996]

G.L.J.A. Rikken and B.A. van Tiggelen, 1996, Observation of Magneto-Transverse Light Diffusion, Nature(London) **381**, 54–56.

Rivas, Sprik, Lagendijk, Noordam, and Rella [2000]

J.G. Rivas, R. Sprik, A. Lagendijk, L.D. Noordam, and C.W. Rella, 2000, Mid-infrared scattering and absorption in Ge powder close to the Anderson localization transition, Phys. Rev. E **62**, R4540–4543.

Rivas, Sprik, Lagendijk, Noordam, and Rella [2001]
J.G. Rivas, R. Sprik, A. Lagendijk, L.D. Noordam, and C.W. Rella, 2001, Static and dynamic transport of light close to the Anderson localization transition, Phys. Rev. E **63**, 046613 (1–12).

Scheffold, Härtl, Maret, and Matijević [1997]
F. Scheffold, W. Härtl, G. Maret, and E. Matijević, 1997, Observation of Long-range Correlations in Temporal Intensity Fluctuations of Light, Phys. Rev. B **56**, 10942–10952.

Scheffold and Maret [1998]
F. Scheffold and G. Maret, 1998, Universal Conductance Fluctuations of Light, Phys. Rev. Lett. **81**, 5800–5803.

Scheffold, Lenke, Tweer, and Maret [1999]
F. Scheffold, R. Lenke, R. Tweer, and G. Maret, 1999, Localization or classical diffusion of light?, Nature (London) **398**, 206–207.

Schuster [1978]
H.G. Schuster, 1978, On a Relation between the Mobility Edge Problem Schuster and an Isotropic XY Model, Z. Phys. **31**, 99–104.

Schuurmans, Megens, Vanmaekelbergh, and Lagendijk [1999]
F.J.P. Schuurmans, M. Megens, D. Vanmaekelbergh, and A. Lagendijk, 1999, Light scattering near the localization transition in macroporous GaP networks, Phys. Rev. Lett. **83**, 2183–2186.

Schuurmans, Vanmaekelbergh, van de Lagemaat and Lagendijk [1999]
F.J.P. Schuurmans, D. Vanmaekelbergh, J. van de Lagemaat, and A. Lagendijk, 1999, Strongly Photonic Macroporous Gallium Phosphide Networks, Science **284**, 141–143.

Sebbah, Hu, Klosner, and Genack [2006]
P. Sebbah, B. Hu, J.M. Klosner, and A.Z. Genack, 2006, Extended Quasimodes within Nominally Localized Random Waveguides, Phys. Rev. Lett. **96**, 183902 (1–4).

Shapiro, Campillo, Stehly, and Ritzwoller [2005]
N.M. Shapiro, M. Campillo, L. Stehly, and M.H. Ritzwoller, 2005, High-Resolution Surface-Wave Tomography from Ambient Surface Noise, Science **307**, 1615–1618.

Skipetrov and van Tiggelen [2004]
S.E. Skipetrov and B.A. van Tiggelen, 2004, Dynamics of Weakly Localized Waves, Phys. Rev. Lett. **92**, 113901 (1–4).

Skipetrov and van Tiggelen [2006]
S.E. Skipetrov and B.A. van Tiggelen, 2006, Dynamics of Anderson localization in open 3D media, Phys. Rev. Lett. **96**, 043902 (1–4).

Snieder, Grêt, Douma, and Scales [2002]
R. Snieder, A. Grêt, H. Douma, and J. Scales, 2002, Coda Wave Interferometry for Estimating Nonlinear Behavior in Seismic Velocity, Science **295**, 2253–2255.

Soukoulis and Datta [1994]
C.M. Soukoulis and S. Datta, 1994, Propagation of classical waves in random media, Phys. Rev. B **49**, 3800–3810.

Sparenberg, Rikken, and van Tiggelen [1997]
A. Sparenberg, G.L.J.A. Rikken, and B.A. van Tiggelen, 1997, Observation of Photonic Magnetoresistance, Phys. Rev. Lett. **79**, 757–760.

Stellmach [1998]
Ch. Stellmach, 1998, Anderson-ocalization and high-frequency induced polarization of ultracold neutrons, PhD thesis, University of Heidelberg.

Stellmach, Abele, Boucher, Dubbers, Schmidt and Geltenbort [2000]
Ch. Stellmach, H. Abele, A. Boucher, D. Dubbers, U. Schmidt and P. Geltenbort, 2000, On the Anderson-localization of ultra-cold neutrons, Nucl. Instr. and Meth. A **440**, 744–749.

Störzer, Gross, Aegerter, and Maret [2006]
M. Störzer, P. Gross, C.M. Aegerter, and G. Maret, 2006, Observation of the critical regime near Anderson localization of light, Phys. Rev. Lett. **96**, 063904 (1–4).

Störzer, Aegerter, and Maret [2006]
M. Störzer, C.M. Aegerter, and G. Maret, 2006, Reduced transport velocity of multiply scattered light due to resonant scattering, Phys. Rev. E **73**, 065602(R) 1–4.

Tsang and Ishimaru [1984]
L. Tsang and A. Ishimaru, 1984, Backscatter enhancement of random discrete scatterers, J. Opt. Soc. Am. A **1**, 836-839.

van Albada and Lagendijk [1985]
M.P. van Albada and A. Lagendijk, 1985, Observation of weak localization of light in a random medium, Phys. Rev. Lett **55**, 2692–2695.

van Albada, van Tiggelen, Lagendijk, and Tip [1991]
M.P. van Albada, B.A. van Tiggelen, A. Lagendijk, and A. Tip, 1991, Speed of propagation of classical waves in strongly scattering media, Phys. Rev. Lett. **66**, 3132–3135.

van der Mark, van Albada, and Lagendijk [1988]
M.B. van der Mark, M.P. van Albada, and A. Lagendijk, 1988, Light scattering in strongly scattering media: Multiple scattering and weak localization, Phys. Rev. B **37**, 3575–3592.

van Tiggelen, Lagendijk, Tip and Reiter [1991]
B.A. van Tiggelen, A. Lagendijk, A. Tip and G.F. Reiter, 1991, Effect of Resonant Scattering on Localization of Waves, Europhys. Lett. **15**, 535–541.

van Tiggelen [1995]
B.A. van Tiggelen, 1995, Transverse Diffusion of Light in Faraday-Active Media, Phys. Rev. Lett. **75**, 422-424.

van Tiggelen, Wiersma and Lagendijk [1995]

B.A. van Tiggelen, D.S. Wiersma and A. Lagendijk, 1995, Self-consistent Theory for the Enhancement Factor in Coherent Backscattering, Europhys. Lett. **30**, 1–7.

van Tiggelen, Lagendijk, and Wiersma [2000]

B.A. van Tiggelen, A. Lagendijk, and D.S. Wiersma, 2000, Reflection and transmission of waves near the localization threshold. Phys. Rev. Lett. **84**, 4333–4336.

Vellekoop, Lodahl, and Lagendijk [2005]

I.M. Vellekoop, P. Lodahl, and A. Lagendijk, 2005, Determination of the diffusion constant using phase-sensitive measurements, Phys. Rev. E **71**, 056604 (1–11).

Vollhardt and Wölfle [1980]

D. Vollhardt and P. Wölfle, 1980, Diagrammatic, self-consistent treatment of the Anderson localization problem in d $\leq$ 2 dimensions, Phys. Rev. B **22**, 4666–4679.

Watson, Fleury, and McCall [1987]

G.H. Watson, P.A. Fleury, and S.L. McCall, 1987, Searching for photon localization in the time domain, Phys. Rev. Lett. **58**, 945–948.

Wiersma [1995]

D.S. Wiersma, 1995, Light in strongly scattering and amplifying random media, PhD thesis, Univ. of Amsterdam.

Wiersma, van Albada, van Tiggelen, and Lagendijk [1995]

D.S. Wiersma, M.P. van Albada, B.A. van Tiggelen, and A. Lagendijk, 1995, Experimental Evidence for Recurrent Multiple Scattering Events of Light in Disordered Media, Phys. Rev. Lett. **74**, 4193–4196.

Wiersma, van Albada, and Lagendijk [1995]

D.S. Wiersma, M.P. van Albada, and A. Lagendijk, 1995, An accurate technique to record the angular distribution of backscattered light, Rev. Sci. Instr. **66**, 5473–5476.

Wiersma, Bartolini, Lagendijk, and Righini [1997]

D.S. Wiersma, P. Bartolini, A. Lagendijk, and R. Righini, 1997, Localization of light in a disordered medium, Nature (London) **390**, 671–673.

Wiersma, Rivas, Bartolini, Lagendijk, and Righini [1999]

D.S. Wiersma, J. Gómez Rivas, P. Bartolini, A. Lagendijk, and R. Righini, 1999, reply to comment "Localization or classical diffusion of light?", Nature (London) **398**, 207.

Wigner [1955]

E.P. Wigner, 1955, Lower Limit for the Energy Derivative of the Scattering Phase Shift, Phys. Rev. **98**, 145–147.

Wolf and Maret [1985]
P.E Wolf and G. Maret, 1985, Weak localization and coherent backscattering of photons in disordered media, Phys. Rev. Lett **55**, 2696–2699.

Wolf, Maret, Akkermans and Maynard [1988]
P.E. Wolf, G. Maret, E. Akkermans, and R. Maynard, 1988, Optical coherent backscattering by random media: an experimental study, J. Phys. (Paris) **49**, 63–75.

Zhu, Pine, and Weitz [1991]
J.X. Zhu, D.J. Pine, and D.A. Weitz, 1991, Internal reflection of diffusive light in random media, Phys. Rev. A **44**, 3948–3959.